Combining EEG and eye movement recording in free viewing: pitfalls and possibilities

Andrey R. Nikolaev*, Radha Nila Meghanathan, Cees van Leeuwen

Laboratory for Perceptual Dynamics, Brain & Cognition Research Unit, KU Leuven - University of Leuven, Leuven, Belgium

* Corresponding author
Laboratory for Perceptual Dynamics,
Brain & Cognition Research Unit,
KU Leuven - University of Leuven,
Tiensestraat 102, Box 3711,
3000 Leuven
Belgium
Tel +32 16 37 32 68
Fax +32 16 32 60 99
Andrey.Nikolaev@kuleuven.be

Abstract

Co-registration of EEG and eye movement has promise for investigating perceptual processes in free viewing conditions, provided certain methodological challenges can be addressed. Most of these arise from the self-paced character of eye movements in free viewing conditions. Successive eye movements occur within short time intervals. Their evoked activity is likely to distort the EEG signal during fixation. Due to the non-uniform distribution of fixation durations, these distortions are systematic, survive across-trials averaging, and can become a source of confounding. We illustrate this problem with effects of sequential eye movements on the evoked potentials and time-frequency components of EEG and propose a solution based on matching of eye movement characteristics between experimental conditions. The proposal leads to a discussion of which eye movement characteristics are to be matched, depending on the EEG activity of interest. We also compare segmentation of EEG into saccade-related epochs relative to saccade and fixation onsets and discuss the problem of baseline selection and its solution. Further recommendations are given for implementing EEG-eye movement co-registration in free viewing conditions. By resolving some of the methodological problems involved, we aim to facilitate the transition from the traditional stimulus-response paradigm to the study of visual perception in more naturalistic conditions.

Keywords: eye tracking, electroencephalography, unconstrained visual exploration, peri-saccadic brain activity, eye-fixation related potentials, saccade-related EEG distortion

1. Introduction

For studying the visual system, two measures that offer excellent temporal resolution are eye tracking and electroencephalography (EEG). The information they provide is complementary: eye tracking can tell us where observers fixate their gaze, and thus where they get their information from; EEG registers how the brain responds to this information. Eye tracking and EEG together, therefore, offer a comprehensive record of the visual system.

The first attempts to study eye movement in combination with EEG were made in the early 1950ies (Evans, 1953; Gastaut, 1951). Research since then has mainly been focused on the immediate consequences of eye movement on the EEG signal (Becker, Hoehne, Iwase, & Kornhuber, 1973; Billings, 1989a; Boylan & Doig, 1989; Csibra, Johnson, & Tucker, 1997; Kazai & Yagi, 1999; Kurtzberg & Vaughan, 1982; Moster & Goldberg, 1990; Riemslag, Van der Heijde, Van Dongen, & Ottenhoff, 1988; Thickbroom, Knezevic, Carroll, & Mastaglia, 1991; Yagi, 1979). Correspondingly, measurement was restricted to activity evoked by single eye movements, within the framework of the traditional stimulus-response paradigm.

More recently, a new generation of video-based eye trackers has widened the use of co-registration of eye movements and EEG (Nikolaev, Pannasch, Ito, & Belopolsky, 2014). In particular, co-registration is increasingly becoming popular in conditions involving continued exploration, i.e., *free viewing*[1]. Because it can be used in naturalistic conditions, co-registration provides an exciting new paradigm for studying attention (Fischer, Graupner, Velichkovsky, & Pannasch, 2013), memory encoding (Nikolaev, Jurica, Nakatani, Plomp, & van Leeuwen, 2013; Nikolaev, Nakatani, Plomp, Jurica, & van Leeuwen, 2011), visual search

[1] Note, that in this paper we use "free viewing" as a shortening for any unconstrained eye movement behavior, regardless of whether this behavior serves any perceptual task or goal. This is different from the narrow usage of "free viewing" to describe visual exploration only, without specific task, as can sometimes be found in the literature.

(Dias, Sajda, Dmochowski, & Parra, 2013; Kamienkowski, Ison, Quiroga, & Sigman, 2012; Kaunitz et al., 2014; Körner et al., 2014), reading (Dimigen, Sommer, Hohlfeld, Jacobs, & Kliegl, 2011; Hutzler et al., 2007), and responses to emotionally charged visual information (Simola, Le Fevre, Torniainen, & Baccino, 2015; Simola, Torniainen, Moisala, Kivikangas, & Krause, 2013), just to mention some domains of basic research in which this technique is successfully being used. In applied research, for instance on brain-computer interfaces, eye movements are used for navigation to a virtual target object, while real-time analysis of the co-registered EEG is used to confirm object selection (Lee, Woo, Kim, Whang, & Park, 2010; Zander, Gaertner, Kothe, & Vilimek, 2011). This paper is intended for researchers who are aiming to contribute to any of these fields, as well as those who want to explore new fields of research with co-registration techniques. Assuming some initial familiarity with either eye tracking or EEG measurement within a stimulus-response paradigm, we will introduce co-registration under free viewing conditions, with particular emphasis on what its pitfalls are and how they could be avoided.

In making the step from the stimulus-response paradigm to free viewing, we need to consider a crucial discrepancy. Traditionally, the EEG signal is segmented according to an external event, usually the onset of the stimulus or the response. Such markers are not available in free viewing. Instead, the eye movements themselves, in particular the saccades, serve as natural markers for EEG segmentation. To enable their use, some issues have to be addressed regarding analysis and interpretation of data. Most of these derive from the fact that eye movements, unlike experimenter-controlled signals in the stimulus-response paradigm, are self-paced and occur in quick succession. As a result, EEG responses evoked by sequential saccades overlap (Dandekar, Privitera, Carney, & Klein, 2012; Dias et al., 2013; Dimigen et al., 2011). This could distort or mask the effects of experimental conditions. Such distortions,

moreover, can easily be mistaken for effects of experimental manipulation. To give a somewhat simplistic example, suppose we are interested in the effect of stimulus size on visual information processing. Inspecting the larger stimulus, however, will require larger saccades. The EEG may differ solely because of larger saccades rather than because of any differences in information processing.

Confounding effects are not always that obvious. For this reason, co-registration should start from an assessment of the liability to confounding of the design chosen. Ideally, eye movements should in all possible respects be equivalent between relevant conditions. In practice, more often the question arises: can we identify a limited set of eye movement characteristics that carries a risk of confounding, and what is the best strategy for controlling it? Which eye movement characteristics are to be controlled will depend on the particular task and experimental goal. For choosing the appropriate strategy, it is important to know which effects eye movements typically have on EEG and in which intervals these effects are typically encountered. Here we will describe the variety of forms these effects can take. This will motivate a solution based on matching eye movement characteristics between conditions. We believe that, in offering solutions to the problems of co-registration in free-viewing conditions, our paper will contribute to making it feasible for a wide scientific community.

1.1. The main peri-saccadic EEG activity

In simultaneous EEG-eye movement analysis, segmentation of EEG into epochs can either be done relative to saccade or to fixation onset, each of which may allow us to capture different aspects of visual processing. Intuitively, activity time-locked to fixation onset may reflect those processes better, which affect perception at the current fixation; whereas, activity time-locked to saccade onset may be better suited for revealing processes related to eye movement

planning and execution. Since either way the epochs comprise the eye fixation interval, their averages are indistinctly called eye-fixation related potentials (EFRP)[2]. Thus, EFRP is a hybrid construct, combining an exploration-driven, eye movement induced signal with a stimulus-driven one, the potential evoked by the visual features at fixation. EFRPs during both controlled and free eye movement behavior have been studied for several decades (Billings, 1989b; Devillez, Guyader, & Guerin-Dugue, 2015; Dimigen et al., 2011; Fudali-Czyz, Francuz, & Augustynowicz, 2014; Kazai & Yagi, 1999; Körner et al., 2014; Nikolaev et al., 2011; Rama & Baccino, 2010; Thickbroom et al., 1991; Yagi, 1979).

Since EFRPs have such a venerable history, we will adopt its terminology for describing the time-frequency EEG activity around a saccade. Accordingly, we will distinguish: the *saccadic spike activity*, named after what is known as the saccadic spike potential and the *lambda activity*, named after the lambda wave/potential. Another important focus will be on the activity that precedes saccade initiation, i.e. *presaccadic activity*.

The *saccadic spike* potential (SP) is a sharp wave at the saccade onset. The SP is elicited even in darkness (Riggs, Merton, & Morton, 1974) as it originates from contraction of extra-ocular muscles during the execution of a saccade (reviewed in Keren, Yuval-Greenberg, & Deouell, 2010). In the frequency domain, the SP is manifested in a range between 20 and 90 Hz (Keren et al., 2010). Consistent with its myogenic nature, the main factors affecting SP amplitude are size (Boylan & Doig, 1989; Keren et al., 2010; Riemslag et al., 1988) and direction of the saccade (Keren et al., 2010; Moster & Goldberg, 1990; Thickbroom & Mastaglia, 1986). Its muscular origin makes the SP an unlikely focus of studies addressing the information processing aspects of visual perception. Yet, the SP plays an important role in co-registration

[2] It would be more exact to distinguish the potentials time-locked to the fixation and saccade onsets by calling them "fixation-related potentials" (FRPs) and "saccade-related potentials" (SRPs), respectively (e.g., Dimigen et al., 2011).

research. Its dependence on saccade size is instrumental in assessing the reliability of various analytical steps, such as the correctness of EEG segmentation and the quality of oculomotor artifact correction, as well as for detecting mismatches between experimental conditions. Thus, the spike potential could be a valuable marker to ensure the adequacy of combined processing of eye movement and EEG.

The *lambda* potential is a positive wave about 100 ms after fixation onset (Evans 1953)[3]. There is common agreement that the lambda potential is a response of the visual cortex to changes in the retinal image due to the saccade (Dimigen, Valsecchi, Sommer, & Kliegl, 2009; Gaarder, Krauskopf, Graf, Kropfl, & Armington, 1964; Kazai & Yagi, 1999, 2003; Riemslag et al., 1988; Thickbroom et al., 1991). In point of fact, the lambda potential is not evoked when saccades are made in darkness or on a homogenous display (Evans, 1953; Fourment, Calvet, & Bancaud, 1976); moreover, the lambda amplitude depends on the difference in luminance between starting and ending locations of the saccade (Ossandón, Helo, Montefusco-Siegmund, & Maldonado, 2010). The association of the lambda potential with early visual processing is confirmed by the similarity in cortical sources of the lambda potential to those of the component P1 in event-related potentials (Kazai & Yagi, 2003). In the frequency domain, the lambda activity is manifested in the upper-theta and alpha bands (6–14 Hz) (Dimigen et al., 2009; Ossandón et al., 2010).

Presaccadic activity is described in EFRP research as a slow positive wave over parieto-occipital brain areas, which starts around 300 ms before saccade onset. This wave has

[3] In the 1970-80ies there has been a long discussion on whether the lambda potential is evoked by saccade or by fixation onset. On the one hand, latency of the lambda potential is time-locked to fixation rather than saccade onsets. This suggests that the lambda potential reflects processes initiated by fixation onset (Billings, 1989a; Yagi, 1979). On the other hand, averaging relative to the saccade and fixation onsets revealed different lambda subcomponents (Thickbroom et al., 1991), suggesting that the lambda potential may be a compound of activity evoked by both saccade and fixation onsets (Kazai & Yagi, 1999; Thickbroom et al., 1991).

sometimes been called the antecedent potential (Becker et al., 1973; Csibra et al., 1997; Kurtzberg & Vaughan, 1982; Moster & Goldberg, 1990; Parks & Corballis, 2008; Richards, 2003). It may co-occur with a positive wave over the frontal areas (Gutteling, van Ettinger-Veenstra, Kenemans, & Neggers, 2010; Richards, 2000). Presaccadic activity may reflect processes related to planning in the visual system, such as oculomotor preparation (Csibra et al., 1997; Kurtzberg & Vaughan, 1982; Richards, 2003), selection and transfer of attention to the next saccade target (Kovalenko & Busch, 2016; Krebs, Boehler, Zhang, Schoenfeld, & Woldorff, 2012; Wauschkuhn et al., 1998), and the anticipatory shift of receptive fields before the saccade ("trans-saccadic remapping") (Parks & Corballis, 2008).

Since attention moves to the target of the next fixation before saccade onset (Hoffman & Subramaniam, 1995), presaccadic activity might indicate reallocation of attention in free viewing. This was, indeed, confirmed in studies operating with a fixation *heat map*. A fixation heat map is a map of the stimulus display wherein the color scale represents the duration and density of fixation. Thus, the color indicates how attractive a region is as a fixation target: the warmer the color, the more attractive the region. When the eyes are moved from cool- to warm-color regions, amplitude of presaccadic activity is larger than vice versa. The presaccadic activity, thus, reflects attention deployed to the next fixation location (Nikolaev et al., 2013). In a multiple target search task, the presaccadic amplitude is more negative for distractors following than preceding the fixation on a target. These results suggest that presaccadic activity reflects memory uptake of target information (Körner et al., 2014). Moreover, presaccadic activity predicts the success of visual short-term memory encoding. At the encoding stage of a free viewing change-detection task, in case change was correctly detected, the presaccadic potential was proportional in amplitude to saccade size; in case of detection failure the amplitude did not correspond to saccade size (Nikolaev et al., 2011). This

implies that change detection failure results from mismatch of saccade and attentional target during visual exploration. Together, these studies illustrate that effects of presaccadic activity can readily be interpreted in relation to visual attention and visual working memory. Since presaccadic activity occurs in a time interval that is crucial for perceptual and cognitive processes involved in saccade guidance, presaccadic activity may be particularly indicative of these processes.

1.2. Eye movement artifacts

Eye movement artifacts are well-known from event-related potential (ERP) studies. In these studies, in order to reduce the number of oculomotor artifacts it is usually sufficient to instruct participants to keep their eyes fixated on a designated location (e.g., the fixation cross) and to refrain from blinking during stimulus presentation[4]. Contaminated trials can then simply be excluded. In case blink or eye movement artifacts remain frequent in the ERP data, correction methods can be used, such as regression (Gratton, Coles, & Donchin, 1983), principal component analysis in combination with dipole modeling (Lins, Picton, Berg, & Scherg, 1993), or independent component analysis (ICA) (Jung et al., 2000). The efficiency of ICA has been proven in hundreds of ERP studies over the last decade, making this technique the most popular one for removal of ocular artifacts. ICA is readily applicable to artifact removal in free viewing conditions.

Because in free viewing, EEG segmentation is determined by saccades, eye movement artifacts are anything but sporadic. The availability of eye tracking information in co-registration is beneficial for ocular artifact detection and correction (Dimigen et al., 2011). Using eye tracking data improves the efficiency of selecting those artifact-related intervals, which are most affected by saccade preparation and execution (Keren et al., 2010; Plöchl,

[4] In that case, participants are asked to blink only in certain intervals, the so called "blink breaks".

Ossandón, & König, 2012). For example, Plöchl and colleagues (2012) proposed a procedure in which the variance of eye movement-related independent components was compared between saccade and fixation intervals defined by eye tracking. In this manner, the corneo-retinal dipole and eyelid artifacts can be eliminated and the saccadic spike activity can be significantly reduced. Yet, even with precise selection of artifact-related components, ocular artifacts cannot be completely separated from neural processes (Plöchl et al., 2012), leaving correction methods at risk of removing activity of interest along with the artifacts.

1.3. Overlapping effects of sequential eye movements on EEG

In free viewing, distortion of EEG signals occurs not only because of oculomotor artifacts. The main problem of simultaneous EEG-eye movement analysis in free viewing is that neural responses to sequential eye movements may overlap. Correspondingly, EEG epochs segmented by saccades may be significantly distorted by activity related to the preceding and the subsequent saccade. Averaging of the epochs relative to the saccade or fixation onsets does not eliminate, or cancel out, this distortion because the distribution of the inter-saccadic intervals, that is, fixation durations, is not uniform. In free viewing, fixation durations have a positively skewed distribution, peaking between 200 and 300 ms (Findlay & Gilchrist, 2003). So the eye movement evoked responses following the current EEG epoch are most likely to occur within this limited interval. Consequently, during averaging of EEG epochs the temporal jitter is not uniform and does not provide the random phase relationships needed for averaging out the activity evoked by preceding or subsequent saccades. This produces a systematic effect in the averaged EEG, which may distort or even mask the effects of perceptual and cognitive processes. Without question, this complication has to be dealt with in order to successfully apply co-registration to free viewing.

The problem of overlapping EEG activity due to eye movement was raised in various domains of study, such as viewing natural scenes (Devillez et al., 2015), visual search (Dandekar, Privitera, et al., 2012; Dias et al., 2013), and reading (Dimigen et al., 2011; Hutzler et al., 2007). Even though these domains have their idiosyncrasies in saccade size, fixation duration, or predominant saccade direction (in particular in reading), the general shape of the fixation duration distribution is the same, and thus the problem of overlapping EEG activity is common between them. The problem is nicely illustrated in the reading study by Dimigen and colleagues (2011): their figure 2B shows how the temporal distribution of preceding and subsequent fixation onsets affects EEG before and after the current saccade. Here, with the saccadic spike activity removed by artifact rejection, the activity that contributes most to the problem of overlap appears to be the lambda responses. Later, we will demonstrate the dominant role of lambda activity in overlapping effects.

Attempts have been made to statistically eliminate distortions due to overlapping EEG responses through linear regression (Dandekar, Privitera, et al., 2012; Dias et al., 2013). Using the general linear model Dandekar and colleagues (2012) built and zeroed out eye movement regressors for five saccade sizes in the interval +/- 492 ms relative to the saccade onset, an interval that included a sequence of approximately three saccades. To remove activity from the interval +/- 3 s relative to the saccade onset, Dias and colleagues (2013) used a method called subspace subtraction. This method is similar to the standard regression approach for ocular artifact correction but considers all EEG and eye movement channels in constructing an optimal estimate of the to-be-removed activity. In contrast to ICA, which identifies activity "blindly" (i.e., without the experimenter's selective intervention) based on a statistical independence assumption, Dias and colleagues (2013) explicitly specified the information

needed to build the regressors: the activity evoked by vertical and horizontal saccades and the saccadic spike potential.

Not only are these procedures mathematically complex and difficult to implement but, more importantly, the linear model may not consider the full variety of factors that contribute to overlapping EEG responses in free viewing. For example, Dandekar and colleagues (2012), whose model considered only saccade size, cautioned that it cannot take into account other factors known to contribute to the lambda response, such as saccade direction or change in luminance between images at saccade onset and offset.

In addition, the linear model is insensitive to the nonlinearity of overlapping EEG responses. Nonlinearity could be accounted for by generalized additive mixed modelling (GAMM), which considers the EEG signal as an additive structure of nonlinear smoothing functions (Tremblay & Newman, 2015; Wood, 2006). Specifically, GAMM combines a parametric part with a non-parametric part, which provides nonlinear smoothing functions for modeling surfaces of two or more numerical predictors. The use of nonlinear regression techniques in modeling eye movement evoked EEG activity is currently in the forefront of co-registration research.

Problems have been raised with the construct validity of regression-corrected factors (Miller & Chapman, 2001): regression involves a predictor variable (the covariate) and an independent variable (the treatment). However, "when the covariate and the treatment are not independent, the regression adjustment may obscure part of the treatment effect or may produce spurious treatment effects" (p. 90, Wildt & Ahtola, 1978). Applying regression in oculomotor behavior runs the risk of violating the assumption of independence because of

sequential dependencies between eye movements. Such dependencies are abundant. For instance, in viewing natural scenes, large saccades have a tendency to be preceded by small saccades; long fixations tend to be followed by long fixations (Tatler & Vincent, 2008). Also trends and long-range dependencies have been reported in eye movements; as an example of the first, extended visual exploration is characterized by decreasing saccade sizes and increasing fixation durations (Unema, Pannasch, Joos, & Velichkovsky, 2005); as an example of the second, the differences in distance and eye position across fixations show the signature 1/f noise, characteristic of memory operating across eye movements (Aks, Zelinsky, & Sprott, 2002). All these dependencies call for caution in applying statistical regression methods to eye movement series.

To avoid potential misuse of statistical regression methods, Miller & Chapman (2001) proposed the solution of matched sampling techniques. In the present context, matching would offer a conservative alternative to regression-based methods. It involves comparing between experimental conditions only those eye movements that are similar in size, direction, and duration. Using this technique instead of regression is the method we will advocate here. Matching of eye movement characteristics has previously been used in free viewing studies (Devillez et al., 2015; Dias et al., 2013; Dimigen et al., 2011; Fischer et al., 2013; Kamienkowski et al., 2012). Dias and colleagues (2013), however, did this in addition to using their subspace subtraction technique to remove saccade-related distortion of EEG. We argue that removing distortion does more harm than good. In our view, since distortion cannot be reliably separated from the EEG signal of interest, it can better be left in the signal. After matching eye movements any saccade-related distortions will be balanced across conditions.

1.4. The scope of the current paper

We will start our survey with a demonstration of the main peri-saccadic EEG activities in two datasets (3.2). We will consider two ways of segmenting EEG: relative to either saccade or fixation onsets (3.3). By comparing the saccade-locked and fixation-locked activity at different EEG frequencies we will show which way of segmenting brain activity of interest is preferable for obtaining the most prominent signal. The distortion of EEG waveforms by eye movements also raises the problem of how to determine a proper interval for baseline correction (3.4). We will consider several possibilities for selection of the baseline interval. We will show how overlapping EEG signals may bias baseline correction and how this problem could be addressed.

Next, we will consider to what extent different eye movement characteristics pose a risk of confounding the EEG signal in free viewing conditions (3.5). We will consider six eye movement characteristics: preceding and current saccade size[5], saccade direction, and duration of the fixations which precede and immediately follow the current saccade. We will demonstrate where and when different eye movement characteristics are at risk of confounding effects on the peri-saccadic EEG.

Even for single eye movements, their characteristics may not be independent of each other. One example we will encounter in this study is the dependency between saccade size and direction. Since saccade sizes tend to be smaller in upward than in other directions (3.5.4), when we observe effects of saccade direction on EEG, the effect may occur indirectly, because of a saccade size difference. More important for free viewing conditions are interdependencies between sequential eye movement characteristics. These may vary, according to the visual task (Tatler & Vincent, 2008).We will show how, for example,

[5] In the simultaneous analysis of EEG and eye movements we prefer to refrain from using "saccade amplitude" even though it is a common term in the eye movement literature. We reserve "amplitude" for EEG measures, thereby avoiding confusion in the description of EEG and eye movements.

interdependency between current saccade size and preceding fixation duration may influence the presaccadic EEG (3.5.3.1).

We will propose a solution to the problem of how to control for overlapping eye movement effects (3.6). For reliable estimation of the saccade-related EEG it is crucial to match the relevant eye movement characteristics across experimental conditions. We will describe a procedure for matching based on the concept of Mahalanobis distance (Dias et al., 2013) and discuss which eye movement characteristics have to be matched to analyze different peri-saccadic activities.

To provide a broad picture of overlapping EEG activity during sequential eye movements we will use the potentials time-locked to the saccade and fixation onsets as well as the time-frequency data in the range from 5 to 45 Hz. This range is commonly studied in perceptual and cognitive research. In the time-frequency domain, we will consider EEG amplitude (power) as well as inter-trial coherence (ITC). ITC indicates synchronization of EEG signals across trials in relation to a phase-locking event. ITC measures only the phase relationship and does not depend on signal amplitude. We will compare the time course of saccade-related changes in terms of power and ITC, and test the effect of the saccade and fixation onset, as phase-locking events, on ITC values.

We will analyze saccade-related epochs corresponding to fixations longer than 200-300 ms (2.5), in order to consider EEG activity uninterrupted by subsequent saccades. This will allow reliable evaluation of the evoked components which correspond to the early components of the ERP. Saccade-related components are commonly viewed as similar to the classical ERP components elicited when stimuli are presented at fixation. Several studies demonstrated this

similarity for the early event-related components P1 and N1 (Belopolsky, Kramer, & Theeuwes, 2008; Graupner, Velichkovsky, Pannasch, & Marx, 2007; Kazai & Yagi, 2003; Ossandón et al., 2010; Rama & Baccino, 2010) as well as the late "cognitive" components such as P300 (Brouwer, Reuderink, Vincent, van Gerven, & van Erp, 2013; Dandekar, Ding, Privitera, Carney, & Klein, 2012; Kamienkowski et al., 2012; but see Dias et al., 2013 for an opposite conclusion) and N400 (Dimigen et al., 2011). In free viewing, the latencies of the early components most likely lie within the duration of a single fixation, whereas the latencies of the late components may only appear after two or even three subsequent saccades. This makes the late components more vulnerable to the issue of overlapping effects than the early ones. In this context it is noteworthy that similarity of the event-related and saccade-related P300 was shown in experiments where either eye movement behavior was controlled (Brouwer et al., 2013; Dandekar, Ding, et al., 2012) or very long fixations in free viewing were selected (Kamienkowski et al., 2012). However, typically, the study of the late components in free viewing is based on the assumption that the perceptual or cognitive processes reflected in these components are not affected by the processes that occur at the onsets of the intervening saccades. There is no way to confirm that this assumption is sound. But even if so, the intervening saccades produce overlapping EEG activity which should be discounted. Matching eye movement characteristics, therefore, is a crucial step for analyzing not only early but also late components. Specifically, when fixation durations are equal, distortions of the current saccade-related activity by the subsequent saccade onsets will be localized in the same interval for the experimental conditions during averaging. Then these distortions can easily be eliminated by matching for characteristics of subsequent saccades and computing the differential activity between the conditions.

2. Methods

We used two datasets of which the perceptual or cognitive implications were, or will be published elsewhere. Here, they served only to illustrate the methodological issues that distinguish a co-registration study from EEG or eye tracking experiments.

Change Blindness (CB) dataset

This dataset was previously used for a study on the perceptual and cognitive processes associated with change blindness (Nikolaev et al., 2013; Nikolaev et al., 2011). Details about the experimental design and procedure could be found in these publications. From the recordings made during the task, here we used the data at the encoding stage. This is when participants freely moved their eyes, looking at and memorizing a photograph of a natural scene (Fig. 1A). In the photograph shown next, a change to the scene was made, which participants were instructed to detect.

Visual Search (VS) dataset

This dataset was obtained for a study of information encoding in visual short-term memory. In a combined visual search-change detection task, participants, first, had to find between 3 and 5 targets among distractors and then, in a subsequent test display, determine whether one of the targets had its orientation changed. Analyses of fixation duration and pupil size as indicators of memory load were published recently (Meghanathan, van Leeuwen, & Nikolaev, 2015); analysis of EEG related to experimental conditions is currently in progress. Here we used EEG-eye movement data from the search display only, which was being inspected prior to the change detection test display (Fig. 1B).

In neither of the datasets was there any restriction on viewing behavior, other than the total time. Both tasks guaranteed that participants had an interest in visually exploring and

memorizing the display. Thus, these data are suitable for demonstrating the intricate effects of eye movements on EEG. The stimulus displays, however, were quite different in character between the two experiments. This led to different patterns of eye movement and EEG. Moreover, differences in EEG recording systems between the two experiments led to differences in EEG analysis. These will be detailed in later sections of this paper; here we indicate the main differences, which may show that to a large degree the datasets were complementary.

Saccade size and fixation duration distributions differed between the two datasets. The proportion of small saccades was larger (Fig. 2A) and fixation durations were longer in the CB than in the VS dataset (Fig. 2B). These differences most likely were due to the nature of the displays, of which the contents had to be memorized. The CB dataset was obtained with color photographs of natural scenes (Fig. 1A), whereas grey fields with relatively small encircled letters were used for the VS dataset (Fig. 1B). The former thus contained a larger amount of high spatial frequencies and a larger range of luminance differences. This necessitated more scrutinizing eye movements: short saccades and long fixations. Therefore, in the CB dataset the minimal fixation duration (and corresponding saccade-related epoch) for inclusion in the analysis was 300 ms, whereas in the VS dataset it was 200 ms (see 2.5 for details). The difference in the displays affected the lambda activity: it was 2-3 times higher in the CB than in the VS dataset, as we will demonstrate below. This most likely occurred because of the larger luminance difference between starting and ending locations of saccades on color photos than on grey displays (Ossandón et al., 2010). Another difference between the datasets was in the EEG recording system: for the CB dataset the EEG was recorded from 15 electrodes, whereas for the VS dataset EEG was recorded from 256 electrodes with a montage

that included peri-ocular channels. This enabled the use of electrooculogram (EOG) in an ocular artifact correction procedure and application of an average reference.

The sections below and the Results section, unless otherwise stated, will describe the CB dataset. The most important differences with the VS dataset will be discussed wherever they arise. Detailed Methods for the VS dataset are described in the Supplementary Materials.

2.1. Participants

19 participants (five male) with normal or corrected-to normal vision took part in the CB experiment. Their median age was 20 (range 19-24). All participants gave written informed consent. The study was approved by the Research Ethics Committee of RIKEN Brain Science Institute (Wako-shi, Japan) where the study was conducted. As we will describe below, here we report the data from 15 participants whose numbers of epochs were sufficient for EEG analysis.

2.2. Stimuli and procedure

48 pairs of color photographs were used as stimuli (Fig. 1A). All were real-world scenes from Rensink et al. (1997). The photographs were pairwise identical, apart from a single detail. This could be the color, position, or presence/absence of an object anywhere in the scene. The images were presented on a 21-inch monitor placed at 85 cm from the participant and had a size of 28° × 22° (width × height). During a trial, the first image of a pair was presented for 20 s. Participants were asked to explore and memorize the image. Then, after a 1-s mask, the second image was presented. Participants were asked to find and indicate the change by clicking a mouse button after placing the cursor on the change region. The second image remained on the screen until response but no longer than 20 s. Feedback was given

immediately after the response by showing the second image again, with a red ellipse encircling the changed region.

2.3. Eye movement recording

Eye movements were recorded with the EyeLink 1000 eye tracking system (SR Research Ltd., Ontario, Canada). The CB experiment used the tower version, which has a chin and forehead rest to stabilize the participant's head. This allows obtaining higher precision of eye positions during visual exploration than the desktop version of the eye tracker. The forehead rest, however, makes it unfeasible to place electrodes for recording an electrooculogram. The VS experiment used the desktop version of the eye tracker and a chinrest, which does not impose any restrictions on placing electrodes around eyes.

Eye tracking was performed with a sampling rate of 500 Hz. We tracked the right eye only. For calibration we used nine points falling in the center, four corners, and the mid-points of the four sides of the screen. The difference between calibration and validation measurement was kept below 1.5°.

2.4. EEG recording

The CB experiment used a Nihon Kohden MEG-6116 amplifier to record EEG with 0.5 Hz high-pass and 100 Hz low-pass online filters and with a 50 Hz notch filter. The sampling rate was 500 Hz. 15 electrodes (F3, F4, C3, C4, P3, P4, O1, O2, T3, T4, T5, T6, Fz, Cz, Pz) were placed according to the international 10-20 system using an ECI electrode cap (Electro-Cap International Inc., Eaton, USA). The ground electrode was FCz. The reference was the linked mastoids.

In the VS experiment, EEG was recorded using a 256-channel Electrical Geodesic System (Electrical Geodesics Inc., Eugene, OR). The electrode montage included channels for recording vertical and horizontal EOGs. During recording the channels were referenced to the vertex electrode (Cz), but in the analysis they were re-referenced to an average reference.

The choice of reference electrode determines the shape of EEG waveforms at each electrode, but not the topographical distribution of EEG amplitude on the scalp surface. Most co-registration studies of free viewing behavior use either a mastoid reference (Devillez et al., 2015; Fischer et al., 2013; Graupner et al., 2007; Körner et al., 2014; Ossandón et al., 2010; Rama & Baccino, 2010; Simola et al., 2015) or an average reference (Dandekar, Privitera, et al., 2012; Dimigen et al., 2009; Kamienkowski et al., 2012). We used a mastoid reference in the analysis of CB dataset because the limited number of electrodes did not allow us to convert the data to average reference reliably (Dien, 1998) and an average reference in the analysis of VS dataset, which was recorded from 256 electrodes.

Synchronization of the eye movement and EEG recordings was achieved as follows. In the CB experiment, the horizontal eye movement coordinate was recorded as an additional channel (the EyeLink channel) along with the regular EEG channels via analog connection between the EyeLink system and the EEG amplifier. A blink-free segment with a length of several seconds was selected in each trial. The lag of maximum correlation was found between the EyeLink channel and the X coordinate time-series from the EyeLink data using normalized cross-correlation (the correlation coefficient was always above 0.98). Then the time stamps of the saccade onsets and offsets were adjusted for this lag and incorporated into the EEG file (see for details Nikolaev et al., 2013). In the VS experiment, a TTL pulse was

sent at the beginning of each trial from the stimulus presentation computer via the parallel port to both eye movement and EEG recording systems.

2.5. Setting limits on eye movement characteristics

Let the "current saccade" be the one on which the given analyses are centered. Relative to its onset or offset (i.e., fixation onset), we considered the preceding fixation and saccade, as well as the subsequent fixation, as schematically depicted above the relevant figures in the Results section.

For eye movement data to be admitted to the analysis, we imposed the following restrictions. The duration of the current saccade had to be smaller than 80 ms[6]. This restriction excluded less than 0.1% of saccades. A saccade was also excluded if a blink occurred within -300 to 300 ms relative to saccade onset (or fixation onset depending on the type of segmentation, as described in "Saccade vs. fixation onset" below). To discount the stimulus onset-related potential, which may last up to 700 ms after stimulus onset (Dimigen et al., 2011), we discarded the first fixation after image onset. Across participants the first fixation had a mean duration of 1473 ms[7] (SD = 451, range - 540-2115 ms). Discarding it, therefore, mostly excluded the activity related to stimulus onset. For fixation duration we set a lower limit at 300 ms and an upper limit at 2000 ms. Whether these limits were imposed on the preceding or subsequent fixation depended on the type of analysis, as specified in Table 1. The limits

[6] As a measure of saccade size we used its duration rather than its length in degrees of visual angle because this makes it easier to understand dependencies between latencies of EEG activities around a saccade. Saccade duration and length are linearly related in a range from 1 to 50 degrees (Leigh & Zee 2006). Within this range, saccade duration can be calculated from saccade length as follows: D = 2.2*L + 21, where D is the saccade duration in ms, and L is the saccade length in degrees (Carpenter, 1988). This formula should serve for most saccades in free picture viewing, which are overwhelmingly within a 2-4 degrees range (Findlay & Gilchrist 2003).

[7] The unusually long duration of the first fixation probably occurred because the trial onset was relatively unexpected for participants since each trial was started by the experimenter, only after the participant maintained stable fixation over a central cross.

removed 59.6% of fixations and increased the mode of fixation duration from 214 to 306 ms and the mean from 307 to 440 ms.

Table 1. Limits on fixation duration for different analyses.

Used in the analyses of	Time-locking event	Preceding fixation duration, ms	Subsequent fixation duration, ms
Current saccade size and direction, preceding saccade size, preceding fixation duration, Saccade vs. fixation onset	Saccade onset	300 < pFD < 2000	No limit
Saccade vs. fixation onset	Fixation onset	300 < pFD < 2000	No limit
Subsequent fixation duration	Fixation onset	No limit	300 < sFD < 2000

Note. "pFD" indicates preceding Fixation Duration; "sFD" indicates subsequent Fixation Duration.

After removing fixations shorter than 300 ms we evaluated the number of intervals which could be used as EEG epochs for each participant. Across all 48 trials there were on average 989 (SD=204, range 543-1343) epochs per participant. As we will describe below, we will typically sort the EEG data into three bins with equal number of saccade-related epochs. To obtain robust EEG estimation, we arbitrarily set the minimal number of epochs per bin to 300, i.e., 900 in total per participant. We excluded four participants who did not reach this criterion and analyzed the EEG-eye movement data from the remaining 15 participants.

2.6. Artifact removal

We analyzed EEG using Brain Vision Analyzer software (Brain Products GmbH, Gilching, Germany). From the 15 recorded channels, we excluded two temporal channels (T3 and T4) because of artifacts resulting from muscle activity. To remove ocular artifacts from EEG we used ICA (Jung et al., 2000). Ocular artifact correction with ICA benefits from using EOG recording, although it is also possible without EOG (Ma, Bayram, Tao, & Svetnik, 2011; Romero, Mananas, & Barbanoj, 2008), as we will discuss in 4.4. EOG was available in the

VS but not in the CB dataset. Consequently, ocular artifact correction of VS dataset involved correlation of ICA components with EOG (see Supplementary Materials), whereas from the CB dataset we subjected 13 regular EEG channels to ICA for artifact correction.

At the first stage, ICA involves selection of a training dataset for computing the unmixing matrix. Following the general rule that for ICA, the more data the better (Onton, Westerfield, Townsend, & Makeig, 2006), we selected as training dataset a 400-s interval after skipping the initial 3 minutes of the experiment. The dataset included several trials of the change detection task. Among the ICA components that were obtained, we identified those which picked up eye movement artifacts as was evident from their time course: these components reflected the blinks and saccades in the EyeLink channel. These components typically had a maximum at the frontal sites, with a characteristic asymmetrical topography corresponding to saccade direction. Blink-related components were identified by their symmetrical maximum at the frontal electrodes. After removing these components the whole EEG signal throughout the session was reconstructed, which led, as expected, mainly to changes in the activity at the frontal sites.

We removed other artifacts, due to large body movements, face/neck muscle activity, poor electrode contact, etc., in the same manner as in ERP studies (Luck, 2005). To this aim, we divided EEG into epochs from -1300 to +1300 ms relative to saccade or fixation onset. At this stage of the analysis, such a long epoch duration was needed to avoid the marginal effects of wavelet transformation, considering that our lowest frequency of interest was 5 Hz (see 2.7). The artifacts were assessed, however, in the interval from -300 to 300 ms around saccade or fixation onset. We rejected EEG epochs if the absolute voltage difference exceeded 50 μV between two neighboring sampling points (as a threshold for a sudden voltage jump) and if

the amplitude exceeded +100 or -100 μV within an epoch (as a threshold for a slow drift). Afterwards the mean number of epochs per bin was 332 (SD= 46; range 272-426) for segmentation relative to saccade onset and 340 (SD= 44; range 283-429) for segmentation relative to fixation onset[8].

2.7. EEG analysis

The EEG data were analyzed only from the 20 s presentations of the first display, when participants visually explored a photograph of a natural scene in order to memorize it.

We estimated the time-frequency structure of the EEG epochs using two-cycle Morlet complex wavelets for 10 logarithmically-spaced center frequencies in the range from 5 to 45 Hz. Having a small number of wavelet cycles permits estimating EEG power and phase in short time windows, albeit at the expense of frequency resolution (Alexander, Trengove, Wright, Boord, & Gordon, 2006). The wavelet duration was 127 ms at 5 Hz and 14 ms at 45 Hz. The wavelets were normalized to have unit scale power to sample rate. After wavelet transformation, the epoch duration was reduced to -300+300 ms relative to a segmentation event. We extracted absolute power and phase. For the power we computed the natural logarithm to approximate the normal distribution. In the CB dataset only, the phase was used for computing inter-trial coherence (ITC) (Delorme & Makeig, 2004), aka the phase-locking factor (Tallon-Baudry, Bertrand, Delpuech, & Pernier, 1996). ITC allowed us to evaluate phase-locking of EEG signals to saccade and fixation onsets across EEG epochs. ITC was calculated as proposed by Delorme and Makeig (2004):

$$ITC(f,t) = \frac{1}{n}\sum_{k=1}^{n}\frac{F_k(f,t)}{|F_k(f,t)|}$$

[8] The numbers differ slightly because the 600-ms epoch interval was shifted by the duration of the intervening saccade (up to 80 ms) and artifacts near the edges of an epoch may appear within an epoch in one way of segmentation but not in another.

where n indicates the number of trials, $F_k(f, t)$ is the Fourier component of trial k at frequency f and time t, estimated by Morlet wavelets. ITC values vary between 0 and 1, where 0 indicates no phase-locking and 1 indicates perfect phase-locking.

For analysis of the saccade-related potentials the EEG signal was filtered with a Butterworth zero-phase filter with a high cut-off frequency of 45 Hz, 12 dB/oct. EEG was segmented into epochs from -300 to +300 ms relative to the segmentation event. The epochs were averaged relative to the saccade or fixation onsets. The averaged potentials, as well as the power and ITC curves, were baseline corrected by subtracting a mean in the interval -300-250 ms before the saccade or fixation onsets, unless otherwise stated.

To measure EEG power for an interval at a given frequency we extracted the mean values over the interval. To measure the saccadic spike and lambda potentials we extracted peak-to-peak amplitudes. For the saccadic spike potential the peak-to-peak amplitude was the difference between positive and negative peak values. For the lambda potential the peak-to-peak amplitude was the difference between the peak value of the lambda potential and the preceding negative peak of the saccadic spike potential. The peak-to-peak amplitude measure has the advantage that it is baseline independent. As we will discuss below (3.4), this is important because baseline selection is complicated in co-registration analysis.

For statistical analysis, unless otherwise stated, we used pointwise t-tests and repeated-measures ANOVA with the Huynh-Feldt correction of p-values associated with two and more degrees of freedom, in order to compensate for violation of sphericity. The obtained p-values were corrected for multiple comparisons using false discovery rate (FDR) (the version

proposed by Storey (2002) and implemented in the *qvalue* package for R). For post-hoc comparison we used the Tukey HSD test.

3. Results

3.1. Eye movements

Saccade duration had a bimodal distribution for both datasets (Fig. 2A), with a mode of 22 ms for the CB dataset and 24 ms for the VS dataset. The CB dataset had a larger number of small (shorter than 20 ms) saccades than the VS dataset. This most likely occurred because of the properties of the displays: since we used photos of natural scenes in the CB experiment versus homogenous displays with sparsely placed letters in the VS experiment, the former contained larger amount of high spatial frequencies than the latter.

Fixation durations were considerably longer in the CB than in the VS dataset (Fig. 2B): a mode of 214 vs. 164 ms and a mean of 307 vs. 197 ms. This is also a most likely consequence of the display difference because scrutiny of photos of natural scenes with a larger range of luminance differences requires longer fixations than search for sparse letters on a homogenous background.

We did not observe a substantial difference in saccade directions between the two datasets (Fig. 2C). Both showed a prevalence of horizontal over vertical saccade directions, as is typical for free viewing behavior (Tatler & Vincent, 2008).

3.2. EEG activity around a saccade

The grand averages of the saccade-related potentials, EEG power, and ITC from the CB dataset are shown in Fig. 3. Those from the VS dataset are shown in Fig. 4. EEG power increased at the latency of the *saccadic spike* potential (around the saccade onset); most prominently at frequencies from 17 Hz and higher (Fig. 3A, 4B, E). The saccadic spike activity may propagate to higher EEG frequencies, up to 90 Hz (Keren et al. 2010), which, however, are out of the scope of our current analysis. ITC went up along with the power increase (Fig. 3B). Saccadic spike amplitude and power were more prominent when time-locked to the saccade (Fig. 4B) rather than to the fixation (Fig. 4E) onset. The saccadic spike potential in the CB dataset (which used a mastoid reference) showed a biphasic wave, which had the same polarity across all electrodes (Fig. 3A), similarly to the data with a nose reference reported by Plöchl et al. (2012, their Fig. 6A). By contrast, the polarity of the potentials in the VS dataset (which used an average reference) was inverted at the anterior areas relative to the posterior areas (see the map at 8 ms in Fig. 4A), consistently with previous observations for average referenced data (Fig. 6B in Plöchl et al., 2012; Keren et al., 2010). Notably, the saccadic spike activity is prominently visible, particularly for the CB dataset, despite the application of ICA for artifact removal. This corresponds to previous observations that even though ICA may completely remove artifacts due to eyelid and eyeball movements, it does not eliminate the saccadic spike potential (Plöchl et al., 2012). The smaller amplitude and power of the saccadic spike activity in the VS than in the CB dataset is a benefit of including EOG channels when using ICA for artifact correction.

At the latency of the *lambda* wave (about 130 ms after saccade onset and 100 ms after fixation onset), there was an increase in EEG power in the 5-28 Hz frequency range, most prominently around 10 Hz (Fig. 3A, 4B, E). The change in ITC at the lambda peak is similar to that of the power (Fig. 3B). Both amplitude and power maps indicate a maximum of

lambda activity over the typical occipital areas (Fig. 4A, C, D, F). These observations are in line with the prominence of lambda activity in the alpha band (Dimigen et al., 2009; Ossandón et al., 2010). The latency of the lambda activity underscores the close link between the lambda potential and the early visual ERP component P1 (Kazai & Yagi, 2003). Also their frequencies correspond: lambda activity is maximally prominent around 10 Hz, while P1 may be an effect of ongoing alpha activity undergoing a phase reorganization (Klimesch, Sauseng, & Hanslmayr, 2007). Phase resetting time-locked to saccade onset in V1 was observed in animal studies (Ito, Maldonado, Singer, & Grün, 2011; Rajkai et al., 2008). Here, phase resetting was confirmed by the increased ITC at the lambda latency over the occipital areas (Fig. 3B).

Amplitude and power of the lambda activity were about 2-3 times higher in the CB than in the VS dataset (cf. Fig. 3A and 4B). This is a likely consequence of different low-level visual properties of the displays used in the experiments: color photos vs. grey fields with sparse letters. Correspondingly, the luminance difference between the starting and ending saccade locations is larger in the CB than in the VS dataset. The luminance difference is known to be proportional to the lambda amplitude (Ossandón et al., 2010).

In the *presaccadic* interval (about -200-20 ms before the saccade), over the occipital areas, the saccade-related potentials time-locked to the saccade onset showed a positive wave which was followed by a negativity, which persisted until the saccadic spike potential (Fig. 3A, 4B). This negativity corresponded to a decrease in power of the EEG signal at low frequencies (5-10 Hz). ITC, on the other hand, showed an increase in the same interval (Fig. 3B). These temporal changes occur because lambda activity evoked by the preceding saccade distorts the current presaccadic activity. The parieto-occipital location of these effects (Fig. 4A) supports their association with lambda activity. As we will show below in the section 3.5.2, these

effects disappear once we select preceding fixations of very long duration (i.e., above 550 ms), because in this case the preceding lambda activity occurs outside the current presaccadic interval.

3.3. Saccade vs. fixation onset

In the CB dataset we compared the EEG activity time-locked to either saccade or fixation onsets for the entire range of epochs. The limits on fixation duration (2.5, Table 1) were applied to the preceding fixation duration for both types of time-locking. After artifact and blink rejection the number of epochs was slightly different between saccade and fixation onset-locked activity, as it was explained in the footnote 8. Since the magnitude of ITC depends on the number of trials, we equalized the number of saccade and fixation onset-locked epochs by identifying, first, the type of time-locking with the smaller number of epochs and then randomly selecting an equal number of epochs from the other one. Visual inspection of the grand-averaged data suggests that both types of time-locking have similar components, which occur shifted in time because of the intervening saccade (the inset in Fig. 5B). To compare the two types of time-locking directly we estimated the lag. For each participant we measured the lag at the peak power of the saccadic spike activity at 35 Hz. On average, the lag was 32.1 (SD=7.9, range 18-42) ms. We shifted forward the time series of power and ITC related to the fixation onset for the individual lags. Then we used pointwise t-tests to compare both power and ITC at all frequencies between activity time-locked to saccade onset and shifted activity time-locked to fixation onset. The differences between saccade and fixation onset are illustrated for both power and ITC at 5 Hz and 35 Hz in Figs. 5 and 6.

Generally, the time courses of power time-locked to saccade and fixation onsets were quite similar after shift correction (Fig. 5A, B), but three major differences remained (Fig. 5C)[9]. In the presaccadic interval, the power at the low frequencies (5-8 Hz) was lower over the occipital areas when the signal was time-locked to the saccade than when it was time-locked to fixation onset (Fig. 5A, C). At the latency of the saccadic spike potential, the power at the high frequencies (22-45 Hz) was higher when the signal was time-locked to the saccade than to fixation onset, more prominently over the fronto-central regions (Fig. 5B). At the latency of the lambda potential, the power over the occipital areas did not differ between the two types of time-locking. Over the frontal regions, the power at the low frequencies was lower when the EEG signal was time-locked to saccade than to fixation onset (Fig. 5A). This effect occurred in the entire pre- and postsaccadic intervals except around the latency of the lambda activity (Fig. 5C).

In ITC, time courses of both time-locking types were similar for presaccadic and lambda activity (Fig. 6). But at the latency of the saccadic spike activity, for higher frequencies ITC time-locked to fixation onset lagged ITC time-locked to saccade onset (Fig. 6B). In addition, ITC magnitude for the saccadic spike activity was lower when time-locked to fixation than to saccade onset (Fig. 6B, C). The reason is evident: with the former the variability in saccade size produces temporal jitter for the preceding saccadic spike activity; this reduces the phase concentration resulting in decreased ITC magnitude and a delay of its peak. The jitter affected power to a much lesser extent (Fig. 5). We also observed some differences in ITC magnitude at the latencies of the presaccadic and lambda activities which, however, were not systematic across EEG channels.

[9] Fig. 5C shows the intervals of significant difference obtained with FDR corrected p-values from the pointwise ANOVAs across 15 participants; the direction of the differences can be observed in Fig. 5A, B.

Next, we directly compared the time courses of power and ITC for EEG activity time-locked to fixation and saccade onsets. Fig. 7A, B illustrates the time course of power and ITC for three frequencies: 5, 10, and 35 Hz. For all these frequencies, immediately after the baseline (-300-250 ms) the power of the presaccadic activity decreased and ITC increased. These trends occurred because of overlap with the preceding lambda activity: due to the 300-ms limit of fixation duration the preceding saccade onsets were concentrated near the left edge of the epoch. These trends disappear when a larger lower limit to fixation duration is introduced (550 ms), as we will demonstrate in section 3.5.2.

For time-locking to saccade onset, the saccadic spike and lambda activity were characterized by simultaneous power and ITC increases (Fig. 7A). For time-locking to fixation onset, at the latency of the saccadic spike potential the ITC at 35 Hz suddenly dropped before rising again, thereby delaying the ITC peak relative to the power peak. As we explained above, this is a consequence of the jitter in onsets of the saccadic spike activity due to variable saccade size (Fig. 6B). At the latency of the lambda wave, the power peak coincided with the ITC peak (Fig. 7B).

We tested whether the observed discrepancy in the time course of the saccadic spike power and ITC at 35 Hz for EEG activity time-locked to fixation onset depended on electrode position. Fig. 7C shows the peak latencies for the saccadic spike power and ITC for frontal, central, parietal, and occipital areas (latencies from left and right electrodes were averaged). The ITC latency increases across areas, whereas the latency of power remains approximately constant. We computed the lag between power and ITC peak values of the saccadic spike activity at 35 Hz. We ran a repeated measures ANOVA on this lag with the factor Topography (4 levels: frontal, central, parietal, occipital areas). The lag increased ($F(3, 42) =$

4.3, $p = 0.02$, $\varepsilon = 0.82$) from frontal (mean=8, SD=9.8 ms) to occipital (mean=20, SD=13.2 ms) areas. The smaller lag in the frontal than in the occipital sites indicates that EEG phase synchronization across epochs arises earlier in sites closer to the eyes. Increasing ITC peak latencies (Fig. 7C) reveal systematic delays in phase locking across brain regions. The saccadic spike activity is characterized by regions of strong phase consistency across trials which move across the scalp, from anterior to posterior. The mechanism underlying this effect requires further exploration. The lack of a similar effect in the power peak may be due to averaging across epochs, which may obscure latency differences across the scalp (Alexander, Trengove, & van Leeuwen, 2015).

In sum, even though saccade- and fixation-onset time-locked activities were quite similar in their time course (Fig. 5A, B), the former results in larger deviation from baseline than the latter, both for power (Fig. 5C) and ITC (Fig. 6C). The largest difference between saccade and fixation time-locking was observed for the saccadic spike activity. Presaccadic power showed a difference over occipital areas in the low-frequencies around 5-8 Hz (Fig. 5A, C). This suggests that the presaccadic activity should preferably be considered as time-locked to saccade onset. We did not observe any difference between the two ways of segmentation for lambda activity at its typical frequency about 10 Hz and in its typical location over occipital areas. Yet, in light of previous studies showing lambda activity to be more closely associated with fixation than with saccade onset (Billings, 1989a; Yagi, 1979) and the possibility of different lambda subcomponents related to onset of saccade and fixation (Kazai & Yagi, 1999; Thickbroom et al., 1991), we propose that lambda activity should preferably be studied with segmentation relative to fixation onset.

3.4. Selection of a baseline interval

Selection of a baseline interval is a challenge in simultaneous EEG-eye movement analysis because different baselines allow approaching different types of brain processes accompanying free viewing. This means that we need to base our choice of baseline on the process we want to study. Several intervals can be offered as candidates (Fig. 8):

A *common* baseline interval is selected from the period of time before presentation of the stimulus display intended for visual exploration with multiple eye movements, i.e., before the trial onset (Fig. 8A). The common baseline is applied to all saccade-related epochs within one trial. This type of baseline allows investigation of accumulative processes occurring across sequential eye movements, such as memory buildup, changes in attention and effort. But the common baseline may be located too far from the to-be-corrected epochs: between different epochs, fluctuations can shift the ongoing EEG to different degrees. Shifts become more likely, the longer the time interval between the baseline and the epoch, making the baseline correction irregular and, correspondingly, unreliable.

Another option is a baseline which we call *local* (Fig. 8B). This type of baseline is selected from one saccade-related epoch within a limited number of sequential epochs of interest and applied to all these epochs. For example, a local baseline can be selected at the fixation on a target and can be applied to the fixations on several previous and following distractors (Körner et al., 2014). This method provides a common reference point for several sequential processes of interest. In addition, being not too far removed from the processes of interest (as compared to the common baseline), the local baseline is much less affected by slow ongoing fluctuations of EEG. But in general, experimental conditions are rare, in which epochs of interest are close to each other in a trial. This obviates a wide applicability of the local baseline.

An *individual* baseline is selected from within some interval of a saccade-related epoch and applied to the rest of the epoch (Fig. 8C). This type of baseline allows investigation of fast processes that change from one saccade to another, for instance ones that are related to perception at the current location or processes related to saccade guidance, such as attention. Being close to the to-be-corrected epochs (typically within several hundred ms), this baseline provides the most accurate correction and is most commonly used in co-registration research. The individual baseline is typically set before saccade onset (Fischer et al., 2013; Fudali-Czyz et al., 2014; Kamienkowski et al., 2012; Kaunitz et al., 2014; Nikolaev et al., 2013) or briefly (e.g., 0-20 ms) after fixation onset (Rama & Baccino, 2010; Simola et al., 2015). In the latter case, it is supposed that the baseline is free of EEG artifacts related to eye movement execution, whereas activity related to visual processing (e.g., the lambda activity) has not started yet.

Besides many advantages, the individual baseline has a major drawback: it is not exempt from the above-mentioned issue of overlapping EEG responses (1.3). Due to the non-uniform distribution of fixation durations, periods with high concentration of saccade-evoked activity occur at the edges of the EEG epoch. These unavoidably contaminate any baseline interval situated there. The result is that experimental conditions that differ in fixation duration become incomparable. Besides this, the baseline in the presaccadic interval can be distorted if the preceding saccades are different in size between experimental conditions, because of the dependence of the saccadic spike and lambda activity on saccade size. Because of this dependency, the activity evoked by the preceding saccade has a potentially confounding effect on the following activity (which, of course, is presaccadic activity for the current saccade).

We will illustrate the effects of selecting an individual baseline in different intervals in the following sections 3.5.1 and 3.5.2.

The individual baseline can be corrupted, not only by overlapping saccade-related activity but also by activity evoked by the stimulus presentation at the beginning of a trial containing multiple saccade-related epochs. If the saccade-related epochs associated with different experimental conditions are distributed non-uniformly in the course of a trial, the baseline for some of the conditions can become unreliable. This issue was raised by Dimigen and colleagues (2011), who described how elevated brain activity right after stimulus presentation (P300 after the sentence presentation) distorts the baseline for saccade-related epochs in one experimental condition (low-predictability words, which tend to occur earlier in the sentence) but not in another (high-predictability words, which tend to occur later). This prevents comparison of the saccade-related epochs associated with high- and low-predictability words. The suggested remedy was to exclude the saccade-related epochs within the first 700 ms after stimulus presentation, the time needed for stimulus-evoked activity to fade out. This issue could be relevant to our present study, because larger saccade size and shorter fixation duration are typically observed in the beginning of free visual exploration (Findlay & Gilchrist, 2003; Unema et al., 2005). Consequently, when saccade-related epochs are partitioned across bins according to saccade size or fixation duration, the ones associated with large saccades or short fixations have a higher probability of occurring in the interval distorted by stimulus-related activity. To avoid this confounding, in the VS dataset we excluded all saccade-related epochs which started within first 700 ms after stimulus presentation. The analysis of the CB dataset was not affected by this issue because we excluded the first fixation, of which the average duration was long enough (1473 ms) to include all the stimulus-onset related activity.

3.5. The effects of eye movement characteristics on EEG

We now proceed to illustrate how particular differences in eye movements between experimental conditions may distort their effect on EEG. We simulated experimental conditions confounded with particular differences in eye movement as follows. We sorted saccade-related epochs in an ascending order according to the eye movement characteristic of interest and divided the sorted epochs in three equal parts, i.e., each bin contained an equal number of epochs. This yielded a quasi-experimental design, in which each bin mimicked a certain level of confounding by the eye movement characteristic of interest. The eye movement characteristics of interest and their mean values in each of the three bins are provided in Table 2 for the CB dataset and in Table S1 (in Supplementary Materials) for the VS dataset.

Table 2. Means and standard deviations of eye movement characteristics for three bins across 15 participants for CB dataset

	1st bin	**2nd bin**	**3rd bin**
Preceding saccade size	17 (2.3) ms ~0.8°	29 (4.1) ms ~3.6°	47 (3.9) ms ~11.8°
Current saccade size	16 (1.9) ms ~0.8°	28 (3.1) ms ~3.6°	46 (3.8) ms ~11.8°
Preceding fixation duration with limits, ms	326 (3.6)	395 (11.4)	595 (45.8)
Preceding fixation duration, no limits, ms	177 (18.9)	285 (19.4)	483 (33.0)
Subsequent fixation duration, ms	327 (3.6)	400 (11.6)	631 (49.0)

As demonstrated in section 3.3, activity time-locked to saccade onset was similar in its time course to activity time-locked to fixation onsets but the former was more prominent, showing larger deviation from the individual presaccadic baseline. The data time-locked to saccade-onset will therefore be used in most of the results below. Unless otherwise stated, effects are

illustrated with EEG power at 10 Hz. This is the peak frequency of the lambda activity, which, as described in the introduction, is the main contributor to saccade-related distortion of EEG. However, statistical results are reported for the entire 5-45 Hz frequency range.

3.5.1. Effect of preceding saccade size

To study the effect of preceding saccade size on EEG we partitioned epochs into three bins corresponding to small, medium and large saccade size. A repeated-measures ANOVA across 15 participants on the mean power of EEG time-locked to the current saccade onset revealed an effect of preceding saccade size on all peri-saccadic activity. The effect is most prominent over the occipital regions. Fig. 9A shows that the following relationship appears to hold: the larger the size of the preceding saccade, the lower the power. The blue areas in Fig. 9C mark the intervals of significant difference between three bins.

This effect is easily mistaken for genuine, and yet it is entirely an artefact of the methodological choices made in analyzing the data; choices that may have appeared reasonable enough at the time. We had chosen to set the minimal fixation duration to 300 ms. This period happens to correspond to the peak of the fixation duration distribution in free viewing (Henderson & Hollingworth, 1999). Consequently, a large amount of the preceding saccadic spike or lambda activity is accumulated near the left edge of the epoch. Consider that saccade size strongly affects the saccadic spike and lambda activity. Thus, first, the shape of the presaccadic activity is distorted proportionally to the preceding saccade size because a larger lambda wave has a larger descending part. This effect appears in the presaccadic activity as the initial decrease in Fig. 9A lasting from approx. -300 to -100 ms. Second, consider we used as our baseline an interval -300-250 ms before the saccade onset, a standard choice in EFRP research. Because the baseline interval is taken at the height of activity evoked by, and proportional in amplitude to, the preceding saccade, baseline correction pulls

down all the activity after -250 ms, proportionally to the size of the preceding saccade. When we set instead the baseline in the interval -100-50 ms before saccade onset, i.e., an interval in which the preceding lambda activity has already faded, the entire difference disappears (Fig. 9B, D). This immediately makes clear how serious an issue in co-registration is the choice of baseline.

3.5.2. Effect of preceding fixation duration

To analyze the effect of the preceding fixation duration on EEG we partitioned epochs into three bins corresponding to short, medium and long fixation duration. Again we observed a prominent effect of preceding fixation duration on all peri-saccadic activity (Fig. 10A, D). The effect was most noticeable over the occipital areas.

This result, again, illustrates an artifact. Different preceding fixation durations push the preceding lambda activity into different intervals of the presaccadic activity. For short fixations (about 320 ms, Table 2), the preceding saccades occur right before the left edge of a -300+300 ms epoch. Consequently, almost the entire interval containing the preceding lambda activity appears within the presaccadic interval of the current saccade. For medium-length fixations, the duration of the preceding fixation was about 400 ms on average. As a result, the descending slope of the preceding lambda activity appeared in the presaccadic interval. Accordingly, the presaccadic activity appears to go down. For long fixations (about 600 ms), the preceding lambda activity ended long before the left epoch edge and the presaccadic activity is no longer distorted.

Previous reports have shown a concentration of lambda activity in the presaccadic interval after averaging of the saccade-related potentials (Dimigen et al., 2011). The present findings are consistent with this observation. In addition, however, we observe that the difference in

duration of preceding fixation affects, not only the peak lambda frequency at about 10 Hz, but, in fact, a large range of frequencies (Fig. 10D). Similar to those of the preceding saccade size (3.5.1), the current effects also strongly depend on the selection of the baseline. When we set the baseline in the interval -100-50 ms instead of -300-250 ms, again the differences disappear (Fig. 10B, E).

Next, we estimated the effect of preceding fixation duration on the EEG, using a baseline interval 0-20 ms after the fixation onset, similarly to Rama & Baccino (2010) and Simola et al. (2015). In this analysis, EEG was time-locked to fixation onset and the preceding fixation could be of any duration, whereas the subsequent fixation was longer than 300 ms (Table 1). Not unexpectedly, we observed a large difference in presaccadic activity between preceding fixations of different duration. In addition, we found a difference at the lambda frequency about 10 Hz and higher, starting from about 150 ms after fixation onset (Fig. 10C, F).

In the analysis of EEG time-locked to fixation onset it is common to select a baseline interval starting from several hundreds of ms before fixation onset (Fischer et al., 2013; Fudali-Czyz et al., 2014; Kamienkowski et al., 2012). Fig. 10C makes it obvious that such a baseline results in a shift of the post-fixation amplitude, if preceding fixations differ in duration between conditions. Thus, even though the preceding fixations do not have a direct influence on the post-fixation activity, they can affect it via the choice of the baseline.

The preceding lambda activity explains the deviation of the presaccadic power and ITC from the baseline, which is observed for the entire range of fixation durations in Figs. 3 and 7A. These figures were plotted using fixations of all durations within our chosen range of 300-2000 ms. These fixations have a mean duration of 440 ms. This value is close to 395 ms

(Table 2), the mean duration of the preceding fixations of medium-length, corresponding to the second bin in the analysis. This correspondence suggests that presaccadic activity in the entire range of fixation durations can be distorted in a way similar to that by medium-length fixations (the red curve in Fig. 10A).

To test this hypothesis we compared the deviations from the baseline for the minimal limits of preceding fixation duration of 300 ms and of 550 ms[10] (Fig. S1 in Supplementary Figures). The limit of 550 ms was selected because it comprises of saccadic spike and lambda activity, which lasts about 250 ms, leaving enough time for the lambda activity after the preceding saccade to fade out before the baseline interval. The baseline interval itself was chosen at -300-250 ms before the onset of the current saccade. The value of 550 ms was also used as the minimum fixation duration in the visual search study by Kamienkowski and colleagues (2012). Fig. S1 (A, D) illustrates the deviation of the presaccadic power and ITC from baseline for preceding fixations longer than 300 and 550 ms. For fixations longer than 300 ms, the presaccadic power decreased (Fig. S1A, B) and the presaccadic ITC increased (Fig. S1D, E) from the baseline. But neither presaccadic power (Fig. S1A, C) nor ITC (Fig. S1D, F) deviated from baseline when the preceding fixations were longer than 550 ms. This observation indicates that presaccadic activity is unaffected by the preceding fixation duration, only if the presaccadic interval is longer than 550 ms.

In sections 3.5.1 and 3.5.2, we simulated experimental conditions confounded by different preceding saccade sizes or fixation durations. This was achieved by dividing EEG epochs into bins according to increasing values of the respective eye movement characteristics. The

[10] Note that although the mean duration of the long preceding fixations (the third bin in Table 2) was 595 ms, the individual fixations within this bin could be shorter than 550 ms, allowing some of the preceding lambda activity to leak into the current signal. For this reason, in order to exclude the effect of the preceding fixation duration it is not sufficient to check the absence of its effect in the third bin.

effects of our simulated conditions on EEG are extreme cases; they are so prominent that they might appear trivial. However, they are helpful to guide our search for artifacts in actual studies, where confounding by saccade size or fixation duration may be much less evident. For example, decreasing presaccadic power as observed in medium-length fixations (Fig. 10A), or as observed in the entire range of preceding fixation durations with minimal duration of 200-300 ms (Fig. 3A, 4B, S1A), could easily be mistaken for effects of preparing the next saccade. But, as we discussed above, they are only effects of the preceding lambda activity. Moreover, considering the effects reported in the sections 3.5.1 and 3.5.2 helps to build a complete picture of the possible effects of eye movement on EEG in close vicinity of the current saccade. This picture is important to make a judicious selection in which characteristics of the eye movements are relevant for matching (section 3.6).

3.5.3. Effect of current saccade size

Saccade size is, amongst eye movement characteristics, probably the one with the most profound impact on EEG. The amplitude of the saccadic spike potential gradually increases with saccade size (reviewed in Keren et al., 2010). The increase is linear until saccade size reaches 10° (~43 ms) (Boylan & Doig, 1989; Riemslag et al., 1988), beyond which it depends on the initial eye position rather than on saccade size (Plöchl et al., 2012). The lambda potential seems to depend on saccade size even if the size is larger than 10° (Yagi, 1979). This study, however, reported statistical significance of the overall trend, but no post-hoc tests for differences between adjacent bins for saccade sizes above 10°. In the above-mentioned studies, saccades of predetermined sizes and restricted directions only were performed. The effects of saccade size for the full range of saccades occurring in free viewing behavior have not systematically been explored. We report these here for both our datasets. We considered not only saccadic spike and lambda but also presaccadic activity. The saccadic spike and lambda activity were measured and illustrated at the location and frequency of their maximal

prominence, the frontal areas (Fz-FL) at 35 Hz power and the occipital areas (O1-OL) at 5-10 Hz, respectively.

3.5.3.1. Effects in bins with equal number of epochs

We partitioned saccade size into three bins with equal number of epochs, corresponding to small, medium and large size. The boundaries of such bins depend on the participant. The means of three bins are given in Table 2 for the CB dataset and in Table S1 for the VS dataset. The effects of saccade size on the saccade-related potential and EEG power time-locked to saccade and fixation onsets are shown for the CB dataset in Fig. 11 and for the VS dataset in Fig. S2. As expected, the saccadic spike and lambda activity were proportional to saccade size. This dependence was much more prominent in the CB than in the VS dataset.

When time-locked to the *saccade onset*, the peak-to-peak amplitude of the saccadic spike potential increased with saccade size in both the CB dataset ($F(2, 28) = 69.0$, $p < 0.001$, $\varepsilon = 0.78$) (Fig. 11A, C) and in the VS dataset ($F(2, 40) = 25.1$, $p < 0.001$, $\varepsilon = 0.85$) (Fig. S2A, C). The peak-to-peak amplitude of the lambda potential increased with saccade size in the CB dataset ($F(2, 28) = 31.7$, $p < 0.001$, $\varepsilon = 0.73$) (Fig. 11B, C) but not in the VS dataset ($F(2, 40) = 1.9$, $p = 0.16$, $\varepsilon = 0.85$) (Fig. S2B, C). This discrepancy was also observed in power (cf. Fig. 11F and S2F), even though in the VS dataset there was a difference in power at low frequencies (Fig. S2F), which we will explore in 3.5.3.2.

The peak latencies of the lambda potentials were shifted proportionally to the saccade duration (Fig. 11B) (Thickbroom et al., 1991). But this shift was not visible in power (Fig. 11E), probably because of the low temporal resolution of the wavelets at 10 Hz.

In neither of our datasets did we observe an effect of saccade size on the power of the *presaccadic activity* (Fig. 11F, S2F) and on the presaccadic potential in the CB dataset (Fig. 11A, B). In the VS dataset the saccade size effect on the mean amplitude in the -180-20 ms interval was highly significant (the left occipital area, OL: $F(2, 40) = 13.9$, $p < 0.001$, $\varepsilon = 0.91$) (Fig. S2A, B). This effect, however, resulted from an *interdependency* between the preceding fixation duration and the current saccade size: not only saccade size, but also preceding fixation duration increased across the 3 saccade size bins: ($F(2, 40) = 97.2$, $p < 0.001$, $\varepsilon = 0.76$). The effect was similar to the one described in 3.5.2 (Fig. 10A), with the only difference that there the range of the preceding fixation durations was substantially larger than here: cf. the values in Table 2 with the current ones (mean and SD): 257 (14.1) ms; 269 (14.7) ms; 289 (20.3) ms. The current effect of the preceding fixation duration on the presaccadic potential, as in 3.5.2, was mediated by the baseline, as follows. The small saccades correspond to the short preceding fixation durations and therefore the preceding saccadic spike potentials occur close to the left edge of the epoch. This means that the baseline (-200-180 ms) was taken at the peak of the saccadic spike potential. The elevated baseline level pushes up the following lambda wave. This aggravated the distortion of the presaccadic activity by the lambda wave (the blue curve in Fig. S2B). By contrast, large saccades are associated with long preceding fixation durations. Therefore, for the large saccades, the baseline happened to be taken at the trough following the preceding saccadic potential. This resulted in a low baseline level and in a lower lambda activity (here imposed on the presaccadic activity, the green curve in Fig. S2B). When we took the baseline in the interval -70-50 ms before the saccade, the saccade size effect on the presaccadic potential disappeared ($F(2, 40) = 0.2$, $p = 0.8$).

When time-locked to *fixation onset*, the peak-to-peak amplitude of the saccadic spike and lambda potentials increased with saccade size in both datasets: the saccadic spike potential in the CB dataset ($F(2, 28) = 14.4$, $p < 0.001$, $\varepsilon = 1.0$) (Fig. 11H, J) and in the VS dataset ($F(2, 40) = 7.6$, $p < 0.002$, $\varepsilon = 1.0$) (Fig. S2H, J); the lambda potential in the CB dataset ($F(2, 28) = 20.1$, $p < 0.001$, $\varepsilon = 0.89$) (Fig. 11I, J) and in the VS dataset ($F(2, 40) = 11.2$, $p < 0.001$, $\varepsilon = 1.0$) (Fig. S2I, J). These increases mainly occurred in the range of small saccades, i.e., between the 1st and 2nd bins rather than between the 2nd and 3rd bins (Tables 2, S1), as between 2nd and 3rd bins there was no significance (all post-hoc $p > 0.5$). The dependency of power on saccade size was observed in all frequencies[11] (Fig. 11K, L, M and S2K, L, M), most prominently in the low frequencies for lambda activity, particularly in the VS dataset (Fig. S2L).

The saccade size effect apparent in the presaccadic interval about 100 ms before the fixation in both datasets (Fig. 11M, S2M) can be understood as an effect of the saccade size effect on the current saccadic spike activity spilling out due to the low temporal resolution of the wavelets at low frequencies.

3.5.3.2. Effects across frequencies

We found a saccade size effect across all EEG frequencies studied (Fig. 11F, M, S2M). Saccadic spike activity is most prominent at frequencies about 60-90 Hz (Keren et al., 2010) and lambda activity is most prominent at frequencies around 10 Hz (Ossandón et al., 2010, Fig. 3A, 4B, E).

[11] At the lambda frequencies (10-22 Hz), about 100 ms after saccade or fixation there was a gap in time, in which we cannot see the saccade size effects (Fig. 11F, M, S2M). This occurred because the ascending slopes of the lambda activity for saccades of different sizes overlapped.

We computed the difference in power between the 3rd and 1st bins for ten frequencies, from 5 to 45 Hz (Fig. 11G, S2G) at the maxima of saccadic spike and lambda power. For saccadic spike activity, the maximum was found over the frontal areas (Fz or FL) in the -100+100 ms interval from saccade onset and for the lambda activity over the occipital areas (O1 or OL) in the 75-200 ms interval from fixation onset. For the saccadic spike activity the power difference was highly significant (all $p < 0.008$, one-sample t-tests against 0) and gradually increased with frequency in both datasets (Fig. 11G, S2G). This finding suggests that the frequencies of maximal prominence of the saccade size effect may correspond to those of the maximal prominence of saccadic spike activity. The latter frequencies, however, lie above the 5-45 Hz range of our study. No such correspondence was observed for the lambda activity: for both datasets the largest difference between the 3rd and 1st bins occurred at the lowest frequency of 5 Hz. For the CB dataset the difference gradually decreased with frequency (Fig. 11G) and was highly significant for all frequencies (all $p < 0.001$, one-sample t-tests against 0). For the VS dataset a difference was observed for 5 Hz ($t(20)=6.5$, $p < 0.001$) and 6 Hz ($t(20)=4.3$, $p < 0.001$), but not above these frequencies (Fig. S2G).

3.5.3.3. Effects of absolute saccade size

The division of saccades into three size bins with equal number of epochs allowed us to consider individual differences in saccade size distributions, because the bin boundaries depend on the participant. To test the effect of absolute saccade size on EEG *irrespective* of individual saccade size distributions, in the CB dataset we partitioned saccade duration into four bins with equal ranges: 0-15, 15-30, 30-45, 45-60 ms (i.e., approximately 0-0.8, 0.8-4, 4-11, 11-18°). The number of epochs was equalized across bins by first identifying the bin with the smallest number of epochs before filling the other three bins with the same numbers of epochs by randomly selecting from the available ones. The dependence on saccade size was

tested for the peak-to-peak amplitude of the saccadic spike and lambda potentials, as well as for the mean power at 35 Hz in the interval from -10 to 30 ms relative to saccade onset for the saccadic spike activity and at 10 Hz in the interval from 100 to 180 ms relative to saccade onset for the lambda activity. Fig. S3 shows the effect of saccade size on the saccade-related potentials and EEG power for the CB dataset.

As expected, the effect of saccade size on the saccadic spike activity was highly significant for the peak-to-peak amplitude ($F(3, 42) = 47.2$, $p < 0.001$, $\varepsilon = 0.67$) as well as power ($F(3, 42) = 41.8$, $p < 0.001$, $\varepsilon = 0.81$) (Fig. S3A-C). The amplitude and power prominently grew across bins up to and including the 3rd bin, which comprised saccades of 30-45 ms duration (~4-11°). In the 4th bin the amplitude and power appeared higher than in the 3rd bin but the post-hoc test showed no significance. The absence of a difference between 3rd and 4th bin is consistent with the observation that for saccades larger than 11.5° the saccadic spike potential does *not* depend on saccade size (Plöchl et al., 2012).

There was a prominent effect of saccade size on the lambda activity for amplitude ($F(3, 42) = 29.0$, $p < 0.001$, $\varepsilon = 0.55$) as well as for power ($F(3, 42) = 16.9$, $p < 0.001$, $\varepsilon = 0.81$) (Fig. S3D-F). The activity prominently grew across bins, up to and including the 3rd bin, appearing even to drop in the 4th bin. Yet the post-hoc test did not show a difference between the 3rd and 4th bins, neither for amplitude nor power, nor between the 1st and 2nd bins for power. Thus, our findings contradict Yagi's (1979) suggestion that the dependency of lambda activity on saccade size extends to saccades larger than 10°.

In sum, both for saccade and fixation time-locking, the saccadic spike and lambda activities strongly depend on saccade size. However this dependency is confined to a relatively limited

range of saccade sizes; it flattens out for larger saccades. For saccadic spike activity the dependency increases with frequency, suggesting correspondence to the frequency of maximal prominence of this activity. By contrast, for the lambda activity the dependency is largest at low frequencies and does not correlate with the frequency of maximal prominence. We did not find an effect of saccade size on the presaccadic activity. We demonstrated, however, that sequential dependency between current saccade size and preceding fixation duration may distort the presaccadic potential via incorrect baseline selection.

3.5.4. Effects of current saccade direction

To study the effect of saccade direction we partitioned the EEG epochs into four saccade direction quadrants: *up*, *down*, *right*, *left*. Saccades, except strictly vertical ones, are lateralized movements, which are reflected in different topography of the saccadic spike activity over the left and right frontal areas (Csibra et al., 1997; Keren et al., 2010; Moster & Goldberg, 1990; Plöchl et al., 2012). We evaluated the peak-to-peak amplitude and the mean power in the –10 +30 ms interval at 35 Hz of the saccadic spike activity at the left and right frontal electrodes (F3-F4 or FL-FR in the CB and VS datasets, respectively). We also evaluated the lambda activity in the left occipital electrode (O1 or OL). For this we obtained the peak-to-peak amplitude and the mean power in the 100-180 ms interval at 10 Hz, as before. Both activities were time-locked to saccade onset. Since we used the mastoid reference in CB dataset but the average reference in VS dataset, the results are presented for the two datasets separately.

For the CB dataset, the amplitude and power of the saccadic spike activity over the left frontal area were smaller for *left* than for *right* saccade directions (all $p < 0.03$, pairwise t-tests) (Fig. 12A, D, G). A tendency to the opposite over the right frontal area (Fig. 12B, E, G) did not reach significance. For *up-down* saccade directions, the amplitude and power over both frontal

areas were larger for the *down* than for the *up* direction (all $p < 0.001$, pairwise t-tests) (Fig. 12A, B, D, E, G). The topography of the saccadic spike activity for the leftward and rightward saccades as well as the larger amplitude for the *down* than for the *up* direction were similar to those found by Plöchl et al. (2012) using a nose reference. However for recordings referenced to the posterior electrodes, larger amplitude has been reported for the *up* than for the *down* direction (Keren et al., 2010; Thickbroom & Mastaglia, 1986).

For the VS dataset, the amplitude and power of the saccadic spike activity over the left frontal areas were opposite to that of the CB dataset: larger for *left* than for *right* saccade directions (all $p < 0.004$, pairwise t-tests) (Fig. S4A, D, G); whereas the amplitude and power over the right frontal areas were larger for the *right* than for the *left* direction (all $p < 0.003$, pairwise t-tests, see Fig. S4B, E, G). The topography was similar to that found using an average reference (Csibra et al., 1997) as well as using a posterior reference (Keren et al., 2010). There was no difference between the *up* and *down* saccade directions.

For the lambda activity, we found no systematic effects of saccade direction, although there was a difference in amplitude of the lambda potential between *up* and *down* directions which, however, was opposite in direction for the CB and VS datasets (Fig. 12C, F and S4C, F) and was not supported by a power difference.

Saccade size and direction can be interdependent (Tatler & Vincent, 2008). Because of this, in principle, saccade size might explain saccade direction effects. We established a relationship between saccade duration and direction in both our datasets: the saccade duration was considerably longer for the *down* than the *up* direction (all $p < 0.001$, pairwise t-tests) (Fig. 12G and S4G), similarly to Tatler and Vincent (2008). This difference corresponded to the

larger amplitude of the saccadic spike activity for the *down* than for the *up* direction in the CB dataset, reported above. Moreover, the saccade duration was significantly longer for the *left* than the *up* direction in both datasets (all $p < 0.002$). However this effect had a counterpart in EEG only over the right frontal area in the CB dataset, and neither over the left frontal area in the CB dataset nor in the VS dataset. These findings indicate that the effects of saccade direction on the saccadic spike activity cannot completely be explained by saccade size. Amplitude and topography of the saccadic spike activity depend on initial eye position rather than on saccade size (Plöchl et al., 2012). This may explain the inconsistent effects of saccade size and direction.

In sum, saccade direction affects amplitude and topographical distribution of the saccadic spike activity. However, the direction of these effects is strongly dependent on the choice of reference electrode. We observed no effect of saccade direction on lambda activity. But since size and direction are correlated, and because saccade size prominently affects the lambda activity, a possible confounding cannot completely be excluded.

3.5.5. Effects of subsequent fixation duration

We tested whether the duration of the subsequent fixation has an effect on the lambda activity and the following postsaccadic activity. Since the lambda wave is time-locked to fixation rather than saccade onset (Billings, 1989a; Yagi, 1979), for this analysis we segmented EEG epochs relative to fixation onset. Also, in contrast to the previous analyses we limited the duration of the subsequent rather than the preceding fixation interval (the effective range of the subsequent fixation duration was 300-2000 ms in the CB dataset and 200-1000 ms in the VS dataset). We partitioned subsequent fixations into three duration bins corresponding to short, medium and long fixation durations (see the means in Table 2 for the CB dataset and in Table S1 for the VS dataset).

In the CB dataset the subsequent fixation duration effect arises in the interval 250-300 ms after the onset of the current fixation (Fig. 13). EEG power at the frequencies 5-17 Hz was higher for shorter than for longer fixation durations (Fig. 13C, E). This effect was observed only in frontal (Fig. 13A, C) and not in occipital (Fig. 13B, D) sites. This means that it cannot be attributed to the lambda activity. Most likely, the effect was related to the initiation of the subsequent saccade, as it occurred over the frontal areas and was most visible for subsequent fixations of short duration (Fig. 13A, C), i.e., when a subsequent saccade started immediately after the end of an epoch. Its occurrence at the low frequencies could be explained as spilling out of subsequent saccadic spike activity, a consequence of the low temporal resolution of low-frequency wavelets. Remarkably, the low-frequency effect at the right edge of the epoch was observed even though a restriction to minimal durations of 300 ms was imposed on epochs carrying the subsequent fixation. Thus, a minimal epoch duration does not secure against effects at the edges of epochs if these epochs differ systematically in fixation duration.

In the VS dataset we did not observe any effects of subsequent fixation duration on EEG (Fig. S5), even though there was a tendency similar to the CB dataset (Fig. 13A, C) at the right edge of the epoch. Consistent with the CB dataset, the tendency suggested higher amplitude for short than for medium and long subsequent fixation durations (Fig. S5A, C).

We conclude that subsequent fixation duration has a small effect at the right edge of an EEG epoch. The effect may play a confounding role in time-frequency analyses involving low-frequency EEG.

3.6. Matching eye movement characteristics before EEG analysis

Averaged saccade-related EEG may be distorted by both saccadic spike and lambda activity from preceding as well as following epochs, because of the non-uniform distribution of fixation durations. Moreover, the presence of sequential dependencies between eye movements (Tatler & Vincent, 2008) suggests that some eye movement characteristics may distort EEG indirectly. Regression-based methods cannot eliminate the distortions, because they can barely be separated from the signal and because of problems in applying regression methods to serially-dependent data. To remedy this problem, we will advocate a strategy of selecting across experimental conditions those EEG epochs that are matched according to their eye movement characteristics (Devillez et al., 2015; Dias et al., 2013; Dimigen et al., 2011; Fischer et al., 2013; Kamienkowski et al., 2012). Matching does not remove the distortions but balances them across conditions. Note, however, that matching is conservative; it may flatten or distort the difference of interest, between perceptual or cognitive processes. This may occur because matching changes distributions of eye movement characteristics and corresponding saccade-related epochs. Since epochs with unmatched characteristics may contain information about the condition in the most conspicuous form, removing such epochs makes information in the remaining epochs more similar between conditions.

The matching procedure we propose involves a selection of eye movements which lie close in a space, in which the dimensionality is defined by the number of characteristics to-be-matched. For example, eye movements may be matched by minimizing the quadratic distance between them in the space of considered characteristics, which is normalized by the sum of their standard deviations (Kamienkowski et al., 2012). Below we will describe a matching procedure which involves finding the Mahalanobis distance across various eye movement characteristics. This procedure was initially proposed by Dias and colleagues (2013), who applied it for equalization across a large set of eye movement characteristics. Their study

involved few targets and numerous distractors. Consequently, they were able to find matches for targets among a large amount of distractors. Such a large difference in number, however, does not usually occur between trials of experimental conditions. As a result, it may be difficult to match all eye movement characteristics. We discuss guidelines for selectively matching eye movement characteristics, depending on the activity of interest in section 4.8.

3.6.1. Matching procedure

Step 1 – Selection of distance measure

The Mahalanobis distance (MD) is a measure of the distance between a data point and the center of the covariance space of a multivariate distribution. This measure can be used to match data points across various eye movement characteristics such as saccade size, fixation duration and saccade direction in two or more experimental conditions. The distributions of eye movement characteristics like saccade size and fixation duration are typically non-normal. In such distributions, the effect of outliers or inflated standard deviations on the MD measure may cause the resultant matching to be unreliable. In that case an alternative is to use the rank-based Mahalanobis distance, wherein effects of non-normality are mitigated. Below we detail the matching procedures based on both of these measures.

Step 2 – Cutoff based elimination

The cutoff distance is selected via an iterative procedure. First, an arbitrary cutoff distance is selected. All data points that lie within this cutoff distance are considered as candidate matched data points. Fig. 14A illustrates this procedure for two experimental conditions across three eye movement characteristics: saccade size, fixation duration and saccade direction. The points that lie above the cutoff distance and, are hence, eliminated, are crossed out. Cutoff distance is reselected if the conditions are not matched (Step 3).

Step 3 – Verification of matching procedure

To verify that the eye movements are successfully matched, we have to show that matched data points have similar eye movement characteristics. This may be done by showing no difference between conditions using a statistical test of significance[12]. If eye movement characteristics are different, the cutoff distance is reduced and Step 2 is repeated. This iterative process of cutoff selection is done until the verification test shows the conditions to be no longer different.

3.6.1.1. Procedure based on Mahalanobis distance

In this procedure, the Mahalanobis distance of each data point (eye movement characteristic) is computed from a reference distribution. This means a reference distribution has to be selected first. The reference distribution may be one of the experimental conditions or a pooled distribution of conditions. If the total number of data points across experimental conditions is *N*, we compute *N* distance measures from the reference distribution. For each multivariate data point, x_i, for $i = 1, \ldots, N$, the MD from the reference distribution with covariance matrix, *S*, and mean, μ, is computed as

$$MD_i = \sqrt{(x_i - \mu)^T S^{-1} (x_i - \mu)}$$

The mean and variance are not ideal measures of the center and spread of the Mahalanobis space, since eye movement characteristics are typically not normal. However, for the purpose of finding data points that lie close to each other across multiple dimensions, selection of the

[12] As it may be argued that not being able to show difference in a statistical test does not mean sameness, we considered a test of equivalence (Wellek, 2010) as an alternative. Equivalence tests are commonly used to show similarity between groups in clinical or pharmaceutical applications. Equivalence tests require the selection of an equivalence interval based on criteria relevant for practical use and the test statistic in use. We found an equivalence test unfit for our matching procedure because of the unavailability of standards or recommendations to establish equivalence of eye movements suitable to our purposes.

appropriate cutoff MD circumvents the problem of non-normality. An appropriate cutoff maybe selected as an arbitrarily high percentile, e.g., 99th, of the distribution of all MDs.

3.6.1.2. Procedure based on rank-based Mahalanobis distance

The rank-based MD (Rosenbaum, 2005) computes the distance between any two data points based on their rank in the distribution. First, the experimental conditions are pooled to give a common distribution of size *N*. Then, each parameter or covariate is replaced by its rank or the average rank in case of ties. For this ranked distribution with covariance matrix, *S*, an adjusted covariance matrix is computed using the formula

$$S_{adj} = R_{diag}\, S\, R_{diag}$$

where R_{diag} is a diagonal matrix of which the diagonal elements are computed as the ratio of the standard deviation of the untied ranks of the covariates to the tied ranks of the covariates. Now, the rank-based MD between any two data points, x_i and x_j, for $i, j = 1, \ldots, N$, in the ranked distribution is computed using the formula

$$MD_{ij} = \sqrt{(x_i - x_j)^T S_{adj} (x_i - x_j)}$$

The total number of distances computed is now (N×(N-1))/2 because the measures are obtained between each data point and every other data point and not between each data point and the distribution. Therefore, after selection of a cut-off value, the elimination procedure is two-step. First, the cutoff is fixed at a high number, e.g., 95. From this two cutoff values are determined – the cutoff MD and the *proximity cutoff*. The cutoff MD is computed as the 95th (cutoff) percentile from all the MDs obtained. The proximity cutoff is computed as 95 (cutoff) percentage of the total number of points from which the distance of each point is calculated, that is, (N - 1)*(cutoff/100). For example, if N = 100, the proximity cutoff is 94 for a cutoff

value of 95. The final set of points are selected as those points that have a rank-based MD less than the cutoff distance from at least as many points as the proximity cutoff.

3.6.1.3. An example application of the matching procedure

We illustrate the matching procedure with an example using high-order properties of the scenes in our CB dataset. The stimulus images were classified according to the *interest* of the observer in the part of the scene subject to change: central or marginal. The classification of each image was determined by Rensink and colleagues (1997), who provided us with the image dataset. For one participant, we compared fixation duration, size and direction[13] of the preceding saccade between these two conditions. The number of eye movements in the central interest condition was 382 (n1) and in the marginal interest condition was 423 (n2). In separate t-tests we found significant differences ($p < 0.05$) for fixation duration and saccade size. Each t-test had a power of 0.8 for a small effect of size $d = 0.2$ (J. Cohen, 1988). Since the data appear non-normal, we additionally confirmed the difference using separate permutation tests. We resampled the data 1000 times using the Monte Carlo method and found the difference between means each time. At the 5% significance level, the conditions were significantly different for fixation duration and saccade size, in agreement with the t-test results.

Data points for computing MD were defined with three eye movement characteristics: fixation duration, saccade size and saccade direction. Saccade direction was included for illustration purposes, even though fixations did not differ on this characteristic between conditions. Data points were then matched across these three characteristics based on both the MD and the rank-based MD. For MD computation, the data points of the *central interest*

[13] To make saccade directions comparable by accounting for circularity, for each saccade, a vector was drawn from the saccade origin to its destination. The cosine transformed slope of this vector was used as a placeholder for saccade direction.

images were used as the reference distribution. The initial cutoff was set at the 99th percentile. The data points that lay above the cutoff were removed. Then we compared the eye movement characteristics of the two conditions for the remaining data points using separate t-tests. If the t-tests found no difference, this result was confirmed by permutation tests to account for the effect of non-normality of the distributions of eye movement characteristics. If either the t-test or the permutation test showed a difference, we reduced the cutoff and repeated the process. Once both tests no longer showed a difference, we stopped the process and considered the eye movement characteristics as matched between conditions. For the rank-based MD, the groups were matched at a cutoff value of 99, while using the MD, matching was attained at a cutoff value of 87[14]. After matching, the number of data points reduced to n1 = 332, n2 = 384 in the rank-based MD procedure and n1 = 299, n2 = 403 in the MD matching procedure. As shown in Fig. 14B, after matching the distributions of the eye movement characteristics are less skewed and more uniform than before.

Power analysis of the t-test on the final set of matched data points showed that a small effect (d = 0.2) could be detected with a probability of 0.76 for MD and 0.74 for rank-based MD. Since the power of the test is close to the recommended 0.8 for detecting even small effects (J. Cohen, 1988), we could assume that the conditions were similar across eye movement characteristics. Thus, in our case there is no advantage of either the MD or rank-based MD. The rank-based MD may be preferable in case of highly skewed distributions, where using MD fails to find a match or results in too small numbers of remaining data points. Generally speaking, the non-normality of eye movement distributions suggests the existence of datasets for which rank-based MD matching could be preferable.

[14] For matching using MD, the cutoff value refers to the (87th) percentile of distances, whereas when using rank-based MD, the cutoff value of 99 refers to both the 99th percentile of distances and 99% used to compute the proximity cutoff.

To verify matching of conditions, a significance test can be used if the sample size is large enough to afford reasonable power (> 0.8) to the test. In the example above, the sample size is very large, so the tests are likely to be overpowered and detect very small effects. Typically, the sample sizes (number of epochs) in EEG analyses are smaller. In the case of a sample size of, e.g., 200 (100 epochs per condition), the power of a t-test would only be 0.3 for detecting small effects (d = 0.2). But, this test still has a power of 0.8 for medium-sized effects (d = 0.4). Therefore, for such sample sizes (200), it is still reasonable to assume conditions to be equal if a t-test shows no statistical difference. For smaller sample sizes, matching cannot be reliably verified using a t-test as it would be underpowered to detect effects of medium size (d = 0.4).

Ideally, in combined EEG-eye movement analyses the effect size optimal for verification of matching should be derived by quantifying the effect of eye movement characteristics on EEG. That is, if a small or medium difference in eye movements (d = 0.2 or d = 0.4) results in changes of EEG within its signal-to-noise ratio, then selection of the effect size can be more liberal (e.g., d = 0.8). However, the choice of an optimal effect size based on the effect of eye movement characteristics on EEG requires meticulous modeling, which should be a subject of future research.

4. General discussion

Co-registration of EEG-eye movement in free viewing conditions has possibilities as well as pitfalls. We examined two datasets which differed in stimulus, task, and EEG recording system, but shared a paradigm involving extensive saccadic exploration of a stimulus display. With these datasets we showed how to analyze evoked potentials, time-frequency decompositions, and inter-trial coherence of the main peri-saccadic EEG activity. We

compared time-locking of EEG segments to the saccade and fixation onsets and discussed different types of baseline correction. However, the major part of our paper was dedicated to the central problem and possible solutions of overlapping EEG responses due to sequential eye movements. Below we will expound our observations and provide some further recommendations for planning and running experiments.

4.1. Stimulus properties

To maximize the benefit of co-registration in free viewing, stimuli should preferably be large. The area within which visual stimuli can be placed (the display area) is limited by the maximal excursion of the eye within the head (the oculomotor range), which is about +/-50°of visual angle (Guitton & Volle, 1987; Stahl, 1999). However, since people tend to start rotating the head when saccades exceed 20° (Fuller, 1992), this value should be the basis for determining maximum display size. Twice this amount (40°), because saccades without head movements could then be made in opposite directions, would be a suitable upper bound for the display size.

If the study is aimed at saccadic exploration of stimuli, the size of each should be larger than the fovea, which has a diameter of about 1° of visual angle around the fixation point (Findlay & Gilchrist, 2003). Spatial separation between stimuli is delimited by visual acuity, which markedly decreases with distance from the fovea. In the parafoveal region (up to 5° of visual angle around the fixation), stimulus information can still be partially processed and encoded (Findlay & Gilchrist, 2003). In natural scenes the size of stimulus region and stimulus separation are beyond the grasp of the experimenter, whereas in artificial displays these can be fully controlled. For example, in the VS experiment, a display item was 0.41° in size and the minimal distance between them was set to 3.12°. Since this distance was still within the

parafoveal region, we encircled each item to complicate discrimination, such that it would require fixation (Körner & Gilchrist, 2007; Peterson & Gibson, 1991). As a result, fixations could unambiguously be attributed to targets or distractors (Meghanathan et al., 2015).

Luminance is another stimulus display property that requires control. Luminance difference between saccadic start and end points may have an effect on lambda activity (Ossandón et al., 2010). Since lambda activity may indirectly (e.g., via baseline, see 3.4) affect the entire peri-saccadic activity, we would recommend that fixation targets have equal luminance. This can easily be achieved for artificial displays but is difficult to obtain with natural scenes. In that case, it should be ensured that luminance at the fixation locations of interest is comparable between conditions.

4.2. Number of trials

In free viewing, observers make about 3-4 saccades per second. During a one-hour experiment one can collect more than 10,000 saccade-related EEG epochs, which might seem more than enough for eliciting robust saccade-related potentials, even if the number of experimental conditions is large. However, in practice, loss of saccade-related epochs during pre-processing is typically much higher in a co-registration study than in a classical ERP study. In addition to classical exclusion factors such as incorrect responses, eye movement and EEG artifacts, exclusion factors specific for co-registration, such as non-target fixations, short fixations (see below) should be taken into account. Moreover, the saccade-related epochs within the first 700 ms after the stimulus onset should be excluded because they may be affected by the stimulus onset-related potential (Dimigen et al., 2011). In addition, we lose the unmatched epochs rejected in the matching procedure we recommended for controlling overlapping effects of sequential eye movements.

The percentage of rejections should be assessed in advance in pilot experiments and pilot analyses. The number of accepted saccade-related EEG epochs per condition should approximately be the same as in ERP studies, because it is generally believed that the main components of the saccade-related potentials are similar to those in ERP. For instance, Luck (2005) recommends having 60 trials for large late components (e.g., P3 or N400), and hundreds of trials for small, earlier components. In co-registration analysis, the saccadic spike potential is already visible after averaging of several tens of epochs. The lambda potential requires averaging of more epochs, which number, however, depends on the luminance range within the stimulus display, as illustrated by the noticeable difference in lambda amplitude between our two datasets. If the matching procedure is applied, a minimum of approximately 100 epochs per condition after rejection is needed to verify matching quality (3.6.1.3).

4.3. Synchronization of stimulus presentation and EEG-eye movement recordings

A typical EEG-eye movement co-registration setup consists of three components: a computer with a monitor for stimulus presentation, an EEG recording system and an eye tracking system. Synchronization of events across these three components, via markers, is a crucial step in the preparation of a co-registration study. Since synchronization markers cannot be inserted after the recording, the researcher has to ascertain beforehand the proper functioning of the synchronization of all components. There are several methods for achieving this.

The most straightforward and reliable way is a common trigger which is sent as a TTL pulse from the presentation computer simultaneously both to the EEG and eye tracking systems. This requires a splitter connected to a parallel port output of the presentation computer[15]. We

[15] Note, however, that modern computers often no longer have an inbuilt parallel port and hence a parallel port card may have to be additionally installed.

used this method in recording the VS dataset. Due to slow drift of the component clocks, during a one-hour experiment, the difference between clocks may reach several hundreds of milliseconds. A single TTL pulse at the beginning is not sufficient for avoiding desynchronization during the experiment. Instead, a TTL pulse should be sent at the onset of every single trial, to keep the difference between the clocks small enough, typically in the order of 1-2ms for a 10s trial.

The second synchronization option involves the output of the eye tracking system. Eye position is typically output as an analog voltage. Via a digital-to-analog converter, it is fed to the EEG recording system, where it appears as a separate channel in the recording. We applied this method of synchronization for the CB dataset.

Thirdly, the growing popularity of EEG-eye movement co-registration has recently led major producers of EEG and eye tracking equipment to develop synchronization tools for their systems. For example, Electrical Geodesics Inc. (Eugene, OR) offers a timing device called "Network Time Protocol". This mechanism allows streaming of stimulus markers and eye movement events directly into the EEG recording software in an online fashion via TCP/IP communication.

Since synchronization of events is achieved via markers sent to the eye movements and EEG systems, it is not necessary to record data with the same sampling rate for both systems. However, it is recommended that the sampling rates be equalized by downsampling the data with the higher sampling rate, since data processing becomes easier when both EEG and eye tracking data have the same number of data points.

4.4. Inclusion of EOG electrodes

In EEG-eye movement co-registration, when the eye movement signal is collected via eye tracking, EOG recording may seem to be redundant. In fact, however, the eye tracking and EOG information are complementary: eye tracking allows precise detection of the eye events, whereas EOG is helpful as an additional input for ocular artifact correction. In contrast to the traditional ERP study, where EOG is mostly used for correction of blink-related artifacts, with co-registration correction of blink effects on EEG is impractical, because blinks are accompanied by transient downward and nasalward eye movements of about 1-5° (Collewijn, van der Steen, & Steinman, 1985). This may create spurious saccade onset signals, rendering saccade-related EEG segmentation inaccurate. In other words, a blink makes it uncertain whether the pervious fixation interval continues after the blink. Moreover, blinks cause large disturbances in EEG amplitude that take significant time to return it to the baseline. Blinks can easily be identified using eye tracking information. Based on this information, the EEG segments between a blink and both the preceding and the following saccade should thus be removed. For example, we excluded saccades and, correspondingly, saccade-related EEG segments if a blink occurred within -300 to 300 ms relative to saccade onset.

Main artifacts, which should be corrected in co-registration, are produced by rotation of the corneo-retinal dipole and by constriction of ocular muscles. EOG recording is mandatory for correction of these artifacts if the regression-based correction methods are used (Romero et al., 2008). But for methods based on blind source separation, such as Independent Component Analysis (ICA), EOG recording is not strictly necessary, because both EOG and EEG are mixtures of ocular and brain signals. EEG, particularly over the frontal sites, contains a large portion of EOG activity (Ma et al., 2011; Romero et al., 2008). Yet, there is a benefit in having EOG recordings as input to ICA. Correlation of independent components with EOG

may facilitate their attribution to ocular artifacts, which is the main difficulty in ICA-based artifact correction. The advantage of using EOG recordings as input to ICA was illustrated by the smaller amplitude of the saccadic spike activity in the VS dataset, which included EOG electrodes, than in the CB dataset, which did not have them.

4.5. Running a co-registration experiment

Efficient preparation and smooth running of a co-registration experiment is greatly enhanced by the cooperation of two experimenters: one responsible for the EEG recording and another for the eye tracking. While the duty of the EEG experimenter consists mainly in the setup and adjustment of EEG electrodes prior to the experiment, with only monitoring of the recording quality needed during the experiment, the work of the eye tracking experimenter continues throughout its course. Video-based eye trackers require a calibration procedure before eye tracking to compute a calibration model in order to establish where on the screen the participant is fixating. The accuracy of this measurement decreases with time for reasons such as participant head movements and drift, i.e., slow movements of the eyes. Typically, the eye tracking software provides drift correction functionality to adjust the calibration model for drift as long as error values are small. This functionality maybe used before each trial. If error is greater than a threshold value, e.g., 2°, drift correction cannot proceed and calibration has to be repeated. In addition, a mandatory re-calibration should be done every 5 or 10 minutes to avoid large errors caused by drift and/or errors introduced by participant head movements. Therefore, in co-registration experiments it is essential to present trials in blocks, in order to allow for re-calibration breaks every 5-10 min.

4.6. Software

Processing of eye movements and EEG data together has often been done using custom software written in MATLAB, Python or other languages. In the last few years, software packages and modules have been developed to make this task easier. The 'Add Channels' module for processing co-registered data is available as part of BrainVision Analyzer version 2.0.3 and later. Currently, this module accepts eye tracking data from SMI, Tobii, ADL, and SR EyeLink 1000 Plus systems. It allows the synchronization of triggers between EEG and eye tracking data and can also identify eye events like saccades and fixations. For MATLAB users, the EYE-EEG extension for EEGLAB has been developed. This extension not only enables synchronization of EEG and eye tracking data as well as saccade and fixation detection, but also provides additional functions such as data removal based on eye position, the ocular artifact correction procedure proposed by Plöchl et al. (2012) (see 1.2), analysis of saccade-related activity in both the time and frequency domain (http://www2.hu-berlin.de/eyetracking-eeg, Dimigen et al., 2011).

4.7. Excluding segments associated with short fixations

There is no consensus among researchers regarding the exclusion of segments associated with short fixations. Some refrain from excluding them altogether (Dias et al., 2013; Körner et al., 2014; Simola et al., 2015; Simola et al., 2013), others exclude segments associated only with short (50-100 ms) fixations (Devillez et al., 2015; Dimigen et al., 2011; Graupner et al., 2007; Ossandón et al., 2010; Rama & Baccino, 2010), still others exclude segments associated with fixations shorter than the mean of the fixation duration distribution (Fischer et al., 2013; Fudali-Czyz et al., 2014; Nikolaev et al., 2013; Nikolaev et al., 2011), or consider for analysis only segments associated with extremely long (>500 ms) fixations (Kamienkowski et al., 2012; Kaunitz et al., 2014).

Exclusion of short fixations and associated EEG segments aims to meet several important goals, such as estimating perceptual or cognitive processes that are completed within one fixation interval, e.g., allocation of attention to the next fixation target (Hoffman & Subramaniam, 1995). In addition, it may appear that exclusion enables time-frequency analysis which, in order to be reliable, requires a minimum number of EEG cycles. Likewise apparently, it permits "clean" EEG epochs, i.e. epochs that contain neither saccadic spike nor lambda activity evoked by adjacent eye movements. However, as we demonstrated in section 3.5, efforts to achieve these aims through exclusion are moot. Because of the non-uniform distribution of fixation durations, no exclusion criterion can prevent, on the one hand, the left edge of an EEG epoch from being distorted by lambda activity related to the preceding saccade and, on the other hand, the right edge from being distorted by saccadic spike activity related to the subsequent saccade. Thus, exclusion criteria based on fixation duration are not sufficient to reduce the influence of sequential eye movements on EEG.

Another caution about exclusion is the significant loss of data. For example, we lost about 60% of segments when we set the lower limit of fixation duration to 300 ms for the CB dataset and to 200 ms for the VS dataset, resulting in considerable reduction in the power of subsequent statistical analysis. Finally, removing data may impoverish or bias information about perceptual and cognitive processes in the dataset. For instance, short fixations may have a particular role in visual processing: they may occur during a fast initial exploration of the scene (Unema et al., 2005). Eliminating short fixations may, therefore, bar us from studying the dynamics of visual exploration.

Decisions about exclusion could still be motivated by assumptions about the processes of interest. For example, exclusion of short saccade-related epochs will absolutely be necessary

when focusing on visual processes that start around the time of a saccade and finish within a fixation interval, because intervening saccades may disrupt these processes and distort the corresponding EEG activity. Consider, for instance, an experiment which aims to analyze lambda activity as an indicator of early visual processing. A lambda wave has a peak latency of 100 ms after fixation onset and returns to baseline after about 200 ms. If the next saccade starts at 50 ms, the lambda wave will be disrupted. However, exclusion may not be necessary for analysis of high-order processes, which involve sampling and accumulation of information from many locations of a scene and are reflected in the late evoked components. If the fixation durations are matched between conditions, the disturbing effect of intervening saccades on the current EEG segment could be ignored, with constraints discussed in 1.4.

Once the decision to exclude short fixations has been made, the next step is to determine the appropriate minimal fixation duration. If the analysis aims at long EEG epochs for studying late components, it will be unaffected by the choice of threshold. If, however, epochs should in their entirety lay within a single fixation (as in our analyses), the threshold value should be set so as to allow epochs to be as long as possible and retain as large a number of epochs as possible in the dataset. The optimal minimal duration thus should be found to the left side of the peak in the fixation duration distribution. The numerical value depends on fixation duration distribution, which varies according to the task and the display used. Average fixations were longer in the CB dataset than in VS dataset, as typically fixation durations are longer in scene memorization than in visual search tasks (Castelhano, Mack, & Henderson, 2009; Henderson, Weeks, & Hollingworth, 1999) and longer for color photos with many details (i.e., with a wide range of spatial frequencies) than for line drawing (Findlay & Gilchrist, 2003). Low-level properties of the display may also affect fixation duration, such as luminance and contrast (Loftus, 1985; Loftus, Kaufman, Nishimoto, & Ruthruff, 1992). Thus,

for choosing a minimal fixation duration the experimenter is advised to assess the distribution of fixation durations in advance from pilot experiments, and adjust the presentation conditions or task if necessary to elicit longer fixation durations to secure sufficiently long EEG segments.

4.8. Selection of eye movement characteristics for matching

Matching was easily reached in the example given in 3.6.1, which had only three eye movement characteristics and two experimental conditions. Increasing either number would render it progressively more difficult to achieve proper matching and reduce the number of EEG epochs per condition after matching. It is better, therefore, to be parsimonious and include only those characteristics that are likely to have an impact on the EEG activity of interest. We will be able to describe a minimal set of eye movement characteristics that have to be matched for studying pre- or postsaccadic activity, based on our observations.

The main eye movement effects on peri-saccadic EEG, which were described in detail in section 3.5, are summarized in Table 3. The main caution in using this table relates to the selection of the baseline interval. When an individual baseline is used, it is essential to match for the preceding saccade size irrespective of the activity studied. The asterisks mark in the table several effects which strongly depend on baseline selection. But actually, improper baseline selection may introduce any confounding effect.

Table 3. The effects of eye movements on peri-saccadic EEG activity

	Presaccadic activity	**Saccadic spike activity**	**Lambda activity**
Preceding saccade size	+	-*	-*
Preceding fixation duration	+	-*	-*
Current saccade size	-	+	+
Current saccade direction	-	+	-
Subsequent fixation duration	-	-	+ (tail)

*depending on the choice of baseline interval.

In sum, in order to study *presaccadic* activity the experimental conditions have to be matched for the duration of preceding fixation as well as for the size and direction of the preceding saccade. To study *postsaccadic* activity the experimental conditions have to be matched for size and direction of the current saccade as well as for the duration of subsequent fixation. The duration of the preceding fixation should be equal between conditions, if the baseline is selected in the presaccadic or early postsaccadic interval. As we have seen above, it is preferable to time-lock epochs to saccade onset when presaccadic activity is being studied and to fixation onset when postsaccadic activity is being studied. Fig. 15 shows a flowchart to assist decision making during combined EEG-eye movement analysis.

4.9. Merits of frequency vs. time domain analysis

Traditionally, evoked potentials time-locked to the saccade or fixation onsets have been the main tool of co-registration research. However, the frequency components of the saccade-related activity are also of interest, because they may coincide and even be confused with the brain rhythms reflected in the perceptual and cognitive processes under study. A striking example of such confusion was demonstrated in the study of microsaccades: concentration of saccadic spike activity about 300 ms after presentation of a visual stimulus may be mistaken for an increase in gamma activity due to perceptual processing, because the microsaccade rate usually increases in this interval (Yuval-Greenberg, Tomer, Keren, Nelken, & Deouell, 2008). In addition, lambda activity evoked by microsaccades increases the spectral power in the alpha and theta band. The power increase is followed by several cycles of alpha oscillations (Dimigen et al., 2009). These may interfere with ongoing alpha activity of cognitive origin. These observations can be extended to saccades of all sizes because microsaccades and

saccades constitute a continuum in terms of physical characteristics and generation mechanisms (Martinez-Conde, Macknik, Troncoso, & Hubel, 2009).

The filtered evoked potentials and the data in the time-frequency domain are complementary (see chapter 2 in Cohen (2014) for discussion). On the one hand, evoked potentials have excellent temporal resolution. Moreover, the extensive literature collected over 70 years of research has allowed researchers to link the components of evoked potentials to perceptual and cognitive processes and brain structures. On the other hand, reliable estimation of evoked potentials is possible only after averaging of many trials. In the averaging, task-relevant information may be lost (Alexander et al., 2013; Alexander et al., 2015). In contrast, the time-frequency analysis can reliably be done on single trials, which allows to study how experimental stimulation modulates ongoing brain activity. Moreover, in contrast to evoked potentials, of which the origin is often uncertain or consists of a mixture of sources, time-frequency analysis reveals oscillatory brain activity, of which the mechanisms and generators are relatively well-understood from animal and in-vitro experiments. Furthermore, synchrony between oscillations allows evaluation of connectivity between brain areas. The drawback is that time-frequency decomposition reduces the temporal resolution of the analysis. Even though to some degree this reduction can be controlled by the parameters of the decomposition, in general, temporal resolution remains an issue in particular for the lower frequencies.

The phase of an EEG signal may be of considerable interest in the study of saccade-related activity in free viewing, because phase is affected by both visual and oculomotor processes at fixation onset. For example, in free viewing of natural scenes the visually evoked responses superimpose on the ongoing activity and change its phase (Ossandón et al., 2010). But even in

complete darkness, i.e., without visual input, the fixation onset is accompanied by phase resetting in a wide frequency range of oscillations recorded from monkey V1 (Rajkai et al., 2008). In scalp-recorded EEG, phase resetting is manifested in the ITC increase at the lambda latency over the occipital areas (Fig. 3B). Saccade-related phase changes may have the function of synchronizing brain areas, in order to collectively bring them into an optimal state for processing of visual information (Jutras & Buffalo, 2010).

5. Conclusion

Co-registration of EEG and eye movements is a valuable technique for investigating the time course of perceptual and cognitive processes in unconstrained visual behavior. But it does engender a set of specific methodological problems that are due to the systematic effects of sequential eye movements on each other's EEG. These effects could be confused with effects of experimental conditions. We illustrated the diversity of these distortions. Our proposed solution consists in matching the relevant eye movement characteristics across experimental conditions. Matching could be done selectively, aided by the catalogue of distortions we identified. We believe that inserting this simple and intuitive step into the analysis procedure makes it possible to widely apply co-registration of EEG and eye movement in various domains of cognitive neuroscience.

Acknowledgements

The authors were supported by an Odysseus grant from the Flemish Organization for Science (FWO). We thank Chie Nakatani, Peter Jurica, and Gijs Plomp for help in experimentation and initial data processing and David Alexander for valuable suggestions.

References

Aks, D. J., Zelinsky, G. J., & Sprott, J. C. (2002). Memory across eye-movements: 1/f dynamic in visual search. *Nonlinear Dynamics, Psychology, and Life Sciences, 6*(1), 1-25.

Alexander, D. M., Jurica, P., Trengove, C., Nikolaev, A. R., Gepshtein, S., Zvyagintsev, M., et al. (2013). Traveling waves and trial averaging: the nature of single-trial and averaged brain responses in large-scale cortical signals. *Neuroimage, 73*, 95-112.

Alexander, D. M., Trengove, C., & van Leeuwen, C. (2015). Donders is dead: cortical traveling waves and the limits of mental chronometry in cognitive neuroscience. *Cognitive Processing, 16*(4), 365-375.

Alexander, D. M., Trengove, C., Wright, J. J., Boord, P. R., & Gordon, E. (2006). Measurement of phase gradients in the EEG. *Journal of Neuroscience Methods, 156*(1-2), 111-128.

Becker, W., Hoehne, O., Iwase, K., & Kornhuber, H. H. (1973). Cerebral and ocular muscle potentials preceding voluntary eye movements in man. *Electroencephalography and Clinical Neurophysiology. Supplement, 33*, 99–104.

Belopolsky, A. V., Kramer, A. F., & Theeuwes, J. (2008). The role of awareness in processing of oculomotor capture: evidence from event-related potentials. *Journal of Cognitive Neuroscience, 20*(12), 2285-2297.

Billings, R. J. (1989a). The origin of the initial negative component of the averaged lambda potential recorded from midline electrodes. *Electroencephalography and Clinical Neurophysiology, 72*(2), 114-117.

Billings, R. J. (1989b). The origin of the occipital lambda wave in man. *Electroencephalography and Clinical Neurophysiology, 72*(2), 95-113.

Boylan, C., & Doig, H. R. (1989). Effect of saccade size on presaccadic spike potential amplitude. *Investigative Ophthalmology and Visual Science, 30*(12), 2521-2527.

Brouwer, A. M., Reuderink, B., Vincent, J., van Gerven, M. A., & van Erp, J. B. (2013). Distinguishing between target and nontarget fixations in a visual search task using fixation-related potentials. *Journal of vision, 13*(3), 17.

Carpenter, R. H. S. (1988). *Movements of the eyes* (2nd ed.). London: Pion Press.

Castelhano, M. S., Mack, M. L., & Henderson, J. M. (2009). Viewing task influences eye movement control during active scene perception. *Journal of vision, 9*(3), 6 1-15.

Cohen, J. (1988). *Statistical Power Analysis for the Behavioral Sciences* (2nd ed.). Hillsdale, NJ: Lawrence Erlbaum Associates.

Cohen, M. (2014). *Analyzing neural time series data*. Cambridge, Massachusetts MIT Press.

Collewijn, H., van der Steen, J., & Steinman, R. M. (1985). Human eye movements associated with blinks and prolonged eyelid closure. *Journal of Neurophysiology, 54*(1), 11-27.

Csibra, G., Johnson, M. H., & Tucker, L. A. (1997). Attention and oculomotor control: a high-density ERP study of the gap effect. *Neuropsychologia, 35*(6), 855-865.

Dandekar, S., Ding, J., Privitera, C., Carney, T., & Klein, S. A. (2012). The fixation and saccade P3. *PLoS One, 7*(11), e48761.

Dandekar, S., Privitera, C., Carney, T., & Klein, S. A. (2012). Neural saccadic response estimation during natural viewing. *Journal of Neurophysiology, 107*(6), 1776-1790.

Delorme, A., & Makeig, S. (2004). EEGLAB: an open source toolbox for analysis of single-trial EEG dynamics including independent component analysis. *Journal of Neuroscience Methods, 134*(1), 9-21.

Devillez, H., Guyader, N., & Guerin-Dugue, A. (2015). An eye fixation-related potentials analysis of the P300 potential for fixations onto a target object when exploring natural scenes. *Journal of vision, 15*(13), 20.

Dias, J. C., Sajda, P., Dmochowski, J. P., & Parra, L. C. (2013). EEG precursors of detected and missed targets during free-viewing search. *Journal of vision, 13*(13), 13.

Dien, J. (1998). Issues in the application of the average reference: Review, critiques, and recommendations. *Behavior Research Methods Instruments & Computers, 30*(1), 34-43.

Dimigen, O., Sommer, W., Hohlfeld, A., Jacobs, A. M., & Kliegl, R. (2011). Coregistration of eye movements and EEG in natural reading: analyses and review. *Journal of Experimental Psychology: General, 140*(4), 552-572.

Dimigen, O., Valsecchi, M., Sommer, W., & Kliegl, R. (2009). Human microsaccade-related visual brain responses. *Journal of Neuroscience, 29*(39), 12321-12331.

Evans, C. C. (1953). Spontaneous excitation of the visual cortex and association areas; lambda waves. *Electroencephalography and Clinical Neurophysiology, 5*(1), 69-74.

Findlay, J. M., & Gilchrist, I. D. (2003). *Active vision*. New York: Oxford University Press.

Fischer, T., Graupner, S. T., Velichkovsky, B. M., & Pannasch, S. (2013). Attentional dynamics during free picture viewing: Evidence from oculomotor behavior and electrocortical activity. *Frontiers in systems neuroscience, 7*, 17.

Fourment, A., Calvet, J., & Bancaud, J. (1976). Electrocorticography of waves associated with eye movements in man during wakefulness. *Electroencephalography and Clinical Neurophysiology, 40*(5), 457-469.

Fudali-Czyz, A., Francuz, P., & Augustynowicz, P. (2014). Determinants of attentive blank stares. An EFRP study. *Consciousness and Cognition, 29*, 1-9.

Fuller, J. H. (1992). Head movement propensity. *Experimental Brain Research, 92*(1), 152-164.

Gaarder, K., Krauskopf, J., Graf, V., Kropfl, W., & Armington, J. C. (1964). Averaged brain activity following saccadic eye movement. *Science, 146*, 1481-1483.

Gastaut, Y. (1951). [A little-known electroencephalographic sign: occipital points occuring during opening of the eyes.]. *Revue Neurologique, 84*(6), 635-640.

Gratton, G., Coles, M. G., & Donchin, E. (1983). A new method for off-line removal of ocular artifact. *Electroencephalography and Clinical Neurophysiology, 55*(4), 468-484.

Graupner, S. T., Velichkovsky, B. M., Pannasch, S., & Marx, J. (2007). Surprise, surprise: two distinct components in the visually evoked distractor effect. *Psychophysiology, 44*(2), 251-261.

Guitton, D., & Volle, M. (1987). Gaze control in humans: eye-head coordination during orienting movements to targets within and beyond the oculomotor range. *Journal of Neurophysiology, 58*(3), 427-459.

Gutteling, T. P., van Ettinger-Veenstra, H. M., Kenemans, J. L., & Neggers, S. F. (2010). Lateralized frontal eye field activity precedes occipital activity shortly before saccades: evidence for cortico-cortical feedback as a mechanism underlying covert attention shifts. *Journal of Cognitive Neuroscience, 22*(9), 1931-1943.

Henderson, J. M., & Hollingworth, A. (1999). High-level scene perception. *Annual Review of Psychology, 50*, 243-271.

Henderson, J. M., Weeks, P. A., & Hollingworth, A. (1999). The effects of semantic consistency on eye movements during complex scene viewing. *Journal of Experimental Psychology: Human Perception and Performance, 25*(1), 210-228.

Hoffman, J. E., & Subramaniam, B. (1995). The role of visual attention in saccadic eye movements. *Perception and Psychophysics, 57*(6), 787-795.

Hutzler, F., Braun, M., Vo, M. L., Engl, V., Hofmann, M., Dambacher, M., et al. (2007). Welcome to the real world: validating fixation-related brain potentials for ecologically valid settings. *Brain Research, 1172*, 124-129.

Ito, J., Maldonado, P., Singer, W., & Grün, S. (2011). Saccade-related modulations of neuronal excitability support synchrony of visually elicited spikes. *Cerebral Cortex, 21*(11), 2482-2497.

Jung, T. P., Makeig, S., Humphries, C., Lee, T. W., McKeown, M. J., Iragui, V., et al. (2000). Removing electroencephalographic artifacts by blind source separation. *Psychophysiology, 37*(2), 163-178.

Jutras, M. J., & Buffalo, E. A. (2010). Synchronous neural activity and memory formation. *Current Opinion in Neurobiology, 20*(2), 150-155.

Kamienkowski, J. E., Ison, M. J., Quiroga, R. Q., & Sigman, M. (2012). Fixation-related potentials in visual search: a combined EEG and eye tracking study. *Journal of vision, 12*(7), 4.

Kaunitz, L. N., Kamienkowski, J. E., Varatharajah, A., Sigman, M., Quiroga, R. Q., & Ison, M. J. (2014). Looking for a face in the crowd: fixation-related potentials in an eye-movement visual search task. *Neuroimage, 89*, 297-305.

Kazai, K., & Yagi, A. (1999). Integrated effect of stimulation at fixation points on EFRP (eye-fixation related brain potentials). *International Journal of Psychophysiology, 32*(3), 193-203.

Kazai, K., & Yagi, A. (2003). Comparison between the lambda response of eye-fixation-related potentials and the P100 component of pattern-reversal visual evoked potentials. *Cognitive, affective & behavioral neuroscience, 3*(1), 46-56.

Keren, A. S., Yuval-Greenberg, S., & Deouell, L. Y. (2010). Saccadic spike potentials in gamma-band EEG: characterization, detection and suppression. *Neuroimage, 49*(3), 2248-2263.

Klimesch, W., Sauseng, P., & Hanslmayr, S. (2007). EEG alpha oscillations: the inhibition-timing hypothesis. *Brain Research. Brain Research Reviews, 53*(1), 63-88.

Körner, C., Braunstein, V., Stangl, M., Schlogl, A., Neuper, C., & Ischebeck, A. (2014). Sequential effects in continued visual search: using fixation-related potentials to compare distractor processing before and after target detection. *Psychophysiology, 51*(4), 385-395.

Körner, C., & Gilchrist, I. D. (2007). Finding a new target in an old display: evidence for a memory recency effect in visual search. *Psychon Bull Rev, 14*(5), 846-851.

Kovalenko, L. Y., & Busch, N. A. (2016). Probing the dynamics of perisaccadic vision with EEG. *Neuropsychologia, 85*, 337-348.

Krebs, R. M., Boehler, C. N., Zhang, H. H., Schoenfeld, M. A., & Woldorff, M. G. (2012). Electrophysiological recordings in humans reveal reduced location-specific attentional-shift activity prior to recentering saccades. *Journal of Neurophysiology, 107*(5), 1393-1402.

Kurtzberg, D., & Vaughan, H. G., Jr. (1982). Topographic analysis of human cortical potentials preceding self-initiated and visually triggered saccades. *Brain Research, 243*(1), 1-9.

Lee, E. C., Woo, J. C., Kim, J. H., Whang, M., & Park, K. R. (2010). A brain-computer interface method combined with eye tracking for 3D interaction. *Journal of Neuroscience Methods, 190*(2), 289-298.

Leigh, R. J., & Zee, D. S. (2006). *The neurology of eye movements* (4th ed.). New York: Oxford University Press.

Lins, O. G., Picton, T. W., Berg, P., & Scherg, M. (1993). Ocular artifacts in recording EEGs and event-related potentials. II: Source dipoles and source components. *Brain Topography, 6*(1), 65-78.

Loftus, G. R. (1985). Picture perception: effects of luminance on available information and information-extraction rate. *Journal of Experimental Psychology: General, 114*(3), 342-356.

Loftus, G. R., Kaufman, L., Nishimoto, T., & Ruthruff, E. (1992). Effects of visual degradation on eye-fixation durations, perceptual processing, and long-term visual memory. In K. Rayner (Ed.), *Eye movements and visual cognition: Scene perception and reading* (pp. 203-226). New York: Springer.

Luck, S. J. (2005). *An Introduction to the Event-Related Potential Technique*. Cambridge, MA: MIT Press.

Ma, J., Bayram, S., Tao, P., & Svetnik, V. (2011). High-throughput ocular artifact reduction in multichannel electroencephalography (EEG) using component subspace projection. *Journal of Neuroscience Methods, 196*(1), 131-140.

Martinez-Conde, S., Macknik, S. L., Troncoso, X. G., & Hubel, D. H. (2009). Microsaccades: a neurophysiological analysis. *Trends in Neurosciences, 32*(9), 463-475.

Meghanathan, R. N., van Leeuwen, C., & Nikolaev, A. R. (2015). Fixation duration surpasses pupil size as a measure of memory load in free viewing. *Frontiers in human neuroscience, 8*, 1063.

Miller, G. A., & Chapman, J. P. (2001). Misunderstanding analysis of covariance. *Journal of Abnormal Psychology, 110*(1), 40-48.

Moster, M. L., & Goldberg, G. (1990). Topography of scalp potentials preceding self-initiated saccades. *Neurology, 40*(4), 644-648.

Nikolaev, A. R., Jurica, P., Nakatani, C., Plomp, G., & van Leeuwen, C. (2013). Visual encoding and fixation target selection in free viewing: presaccadic brain potentials. *Frontiers in systems neuroscience, 7*, 26.

Nikolaev, A. R., Nakatani, C., Plomp, G., Jurica, P., & van Leeuwen, C. (2011). Eye fixation-related potentials in free viewing identify encoding failures in change detection. *Neuroimage, 56*(3), 1598-1607.

Nikolaev, A. R., Pannasch, S., Ito, J., & Belopolsky, A. V. (2014). Eye movement-related brain activity during perceptual and cognitive processing. *Frontiers in systems neuroscience, 8*, 62.

Onton, J., Westerfield, M., Townsend, J., & Makeig, S. (2006). Imaging human EEG dynamics using independent component analysis. *Neuroscience and Biobehavioral Reviews, 30*(6), 808-822.

Ossandón, J. P., Helo, A. V., Montefusco-Siegmund, R., & Maldonado, P. E. (2010). Superposition model predicts EEG occipital activity during free viewing of natural scenes. *Journal of Neuroscience, 30*(13), 4787-4795.

Parks, N. A., & Corballis, P. M. (2008). Electrophysiological correlates of presaccadic remapping in humans. *Psychophysiology, 45*(5), 776-783.

Peterson, M. A., & Gibson, B. S. (1991). Directing spatial attention within an object: altering the functional equivalence of shape descriptions. *Journal of Experimental Psychology: Human Perception and Performance, 17*(1), 170-182.

Plöchl, M., Ossandón, J. P., & König, P. (2012). Combining EEG and eye tracking: identification, characterization, and correction of eye movement artifacts in electroencephalographic data. *Frontiers in human neuroscience, 6*, 278.

Rajkai, C., Lakatos, P., Chen, C. M., Pincze, Z., Karmos, G., & Schroeder, C. E. (2008). Transient cortical excitation at the onset of visual fixation. *Cerebral Cortex, 18*(1), 200-209.

Rama, P., & Baccino, T. (2010). Eye fixation-related potentials (EFRPs) during object identification. *Visual Neuroscience, 27*(5-6), 187-192.

Rensink, R., O'Regan, J., & Clark, J. (1997). To see or not to see: the need for attention to perceive changes in scenes. *Psychological science, 8*, 368-373.

Richards, J. E. (2000). Localizing the development of covert attention in infants with scalp event-related potentials. *Developmental Psychology, 36*(1), 91-108.

Richards, J. E. (2003). Cortical sources of event-related potentials in the prosaccade and antisaccade task. *Psychophysiology, 40*(6), 878-894.

Riemslag, F. C., Van der Heijde, G. L., Van Dongen, M. M., & Ottenhoff, F. (1988). On the origin of the presaccadic spike potential. *Electroencephalography and Clinical Neurophysiology, 70*(4), 281-287.

Riggs, L. A., Merton, P. A., & Morton, H. B. (1974). Suppression of visual phosphenes during saccadic eye-movements. *Vision Research, 14*(10), 997-1011.

Romero, S., Mananas, M. A., & Barbanoj, M. J. (2008). A comparative study of automatic techniques for ocular artifact reduction in spontaneous EEG signals based on clinical target variables: a simulation case. *Computers in Biology and Medicine, 38*(3), 348-360.

Rosenbaum, P. R. (2005). An exact distribution-free test comparing two multivariate distributions based on adjacency. *Journal of the Royal Statistical Society Series B-Statistical Methodology, 67*, 515-530.

Simola, J., Le Fevre, K., Torniainen, J., & Baccino, T. (2015). Affective processing in natural scene viewing: valence and arousal interactions in eye-fixation-related potentials. *Neuroimage, 106*, 21-33.

Simola, J., Torniainen, J., Moisala, M., Kivikangas, M., & Krause, C. M. (2013). Eye movement related brain responses to emotional scenes during free viewing. *Frontiers in systems neuroscience, 7*, 41.

Stahl, J. S. (1999). Amplitude of human head movements associated with horizontal saccades. *Experimental Brain Research, 126*(1), 41-54.

Storey, J. D. (2002). A direct approach to false discovery rates. *Journal of the Royal Statistical Society Series B-Statistical Methodology, 64*, 479-498.

Tallon-Baudry, C., Bertrand, O., Delpuech, C., & Pernier, J. (1996). Stimulus specificity of phase-locked and non-phase-locked 40 Hz visual responses in human. *Journal of Neuroscience, 16*(13), 4240-4249.

Tatler, B. W., & Vincent, B. T. (2008). Systematic tendencies in scene viewing. *Journal of Eye Movement Research, 2*(2).

Thickbroom, G. W., Knezevic, W., Carroll, W. M., & Mastaglia, F. L. (1991). Saccade onset and offset lambda waves: relation to pattern movement visually evoked potentials. *Brain Research, 551*(1-2), 150-156.

Thickbroom, G. W., & Mastaglia, F. L. (1986). Presaccadic spike potential. Relation to eye movement direction. *Electroencephalography and Clinical Neurophysiology, 64*(3), 211-214.

Tremblay, A., & Newman, A. J. (2015). Modeling nonlinear relationships in ERP data using mixed-effects regression with R examples. *Psychophysiology, 52*(1), 124-139.

Unema, P. J. A., Pannasch, S., Joos, M., & Velichkovsky, B. M. (2005). Time course of information processing during scene perception: The relationship between saccade amplitude and fixation duration. *Visual Cognition, 12*(3), 473-494.

Wauschkuhn, B., Verleger, R., Wascher, E., Klostermann, W., Burk, M., Heide, W., et al. (1998). Lateralized human cortical activity for shifting visuospatial attention and initiating saccades. *Journal of Neurophysiology, 80*(6), 2900-2910.

Wellek, S. (2010). *Testing statistical hypotheses of equivalence and noninferiority* (2nd ed.): Chapman and Hall/CRC.

Wildt, A. R., & Ahtola, O. T. (1978). *Analysis of covariance*. Beverly Hills, CA: Sage.

Wood, S. N. (2006). *Generalized additive models*. New York: Chapman & Hall/CRC.

Yagi, A. (1979). Saccade size and lambda complex in man. *Physiological Psychology, 7*, 370-376.

Yuval-Greenberg, S., Tomer, O., Keren, A. S., Nelken, I., & Deouell, L. Y. (2008). Transient induced gamma-band response in EEG as a manifestation of miniature saccades. *Neuron, 58*(3), 429-441.

Zander, T. O., Gaertner, M., Kothe, C., & Vilimek, R. (2011). Combining eye gaze input with a brain-computer interface for touchless human-computer interaction. *International Journal of Human-Computer Interaction, 27*(1), 38-51.

Figure captions

Figure 1**. Examples of** s**timuli used in two free-viewing experiments**. A. An example of a natural scene used in the encoding stage of the change blindness task for the "CB dataset". B. An example of an array containing Ts among Ls used in the multiple-target search stage of the change detection task for the "VS dataset".

Figure 2. **Eye movement characteristics in two datasets: change blindness (CB) and visual search (VS)**. A. Saccade duration. B. Fixation duration. C. Saccade direction.

Figure 3. **CB dataset: main EEG activity around a saccade averaged across 15 participants for 13 scalp electrodes.** A. Saccade-related potentials (red curves, left Y-axis) superimposed on the time-frequency plots of EEG log-power time-locked to saccade onset. B. The time-frequency plots of inter-trial coherence (ITC) relative to saccade onset.

Figure 4. **VS dataset: main EEG activity around saccades averaged across 21 participants.** Activity time-locked to saccade onset is in A-C; activity time-locked to fixation onset is in D-F. A. Evoked potential voltage maps. B. Saccade-related potential (red curve, left Y-axis) superimposed on time-frequency plot of EEG log-power (the scale is indicated by numbers on the contour lines) for activity averaged across seven electrodes over the left occipital area (OL). C. Maps of log-power distribution at specified time points and frequencies. D. Evoked potential voltage maps E. Saccade-related potential (red curve, left Y-axis) superimposed on time-frequency plot of EEG log-power (the scale is indicated by numbers on the contour lines) for activity averaged across seven electrodes over OL. F. Maps of log-power distribution at specified time points and frequencies. In A, C, D, F the left map

shows the mean activity in the presaccadic interval; the central map is taken at the maximum of the saccadic spike activity; the right map is taken at the maximum of the lambda activity.

Figure 5. **CB dataset: Segmentation relative to saccade vs. fixation onsets: power.** A. EEG log-power at 5 Hz time-locked to saccade and fixation onsets *after* shifting in time the fixation-locked activity, in order to compensate for saccade duration. B. The same at 35 Hz. The inset shows EEG log-power at 35 Hz time-locked to saccade and fixation onsets *before* shifting in time. C. Intervals of significant difference between EEG power time-locked to saccade and fixation onsets after the shift.

Figure 6. **CB dataset: Segmentation relative to saccade vs. fixation onsets: ITC.** A. ITC at 5 Hz time-locked to saccade and fixation onsets after shifting the fixation-locked activity. B. The same at 35 Hz. C. Intervals of significant difference between ITC time-locked to saccade and fixation onsets after the shift.

Figure 7. **CB dataset: Time-locking relative to saccade vs. fixation onsets.** A. EEG log-power (left Y axis) and ITC (right Y axis) time-locked to saccade onset for three EEG frequencies in electrode O1. B. The same for activity time-locked to fixation onset. C. Peak latency of power and ITC time-locked to fixation onset at 35 Hz in four brain regions. Error bars indicate standard errors of the means across 15 participants.

Figure 8. P**ossible locations of baseline interval**. Rectangular frames designate trials with duration of several seconds and containing multiple fixations (=saccade-related epochs). Solid bars designate saccade-related epochs. Pink bars designate possible baseline locations. A. A common baseline. B. A local baseline. C. An individual baseline.

Figure 9. **CB dataset: Effect of preceding saccade size on EEG.** A. EEG log-power at 10 Hz in electrode O1, time-locked to saccade onset, in three saccade size bins with equal numbers of epochs for baseline -300-250 ms. C. Intervals of significant difference between bins in A. B-D. The same for baseline -100-50 ms. Pink bars designate baseline locations.

Figure 10. **CB dataset: Effect of preceding fixation duration on EEG**. A. EEG log-power at 10 Hz in electrode O1, time-locked to saccade onset in three fixation duration bins with equal numbers of epochs for baseline -300-250 ms. D. Intervals of significant difference between bins in A. B-E. The same for baseline -100-50 ms. C. EEG log-power at 10 Hz in electrode O1, time-locked to fixation onset in three fixation duration bins with equal numbers of epochs for baseline 0-20 ms. F. Intervals of significant difference between bins in C. Pink bars designate baseline locations.

Figure 11. **CB dataset: Effect of saccade size on EEG**. Activity time-locked to saccade onset is in A-F; activity time locked to fixation onset is in H-M. Error bars indicate standard errors of the means across 15 participants. A. Saccade-related potential time-locked to saccade onset in three saccade size bins with equal number of epochs for electrode Fz. B. The same for electrode O1. C. Peak-to-peak amplitude of the saccadic spike potential ("SP") and difference in amplitude between lambda and negative saccadic spike peaks ("Lambda") for three saccade size bins. D. EEG log-power at 35 Hz time-locked to saccade onset in three saccade size bins with equal numbers of epochs for electrode Fz. E. The same for 10 Hz and electrode O1. F. Intervals of significant difference between three bins. G. Difference in saccadic spike and lambda power between the third and first bin at each frequency in the 5-45 Hz range. H. Saccade-related potential time-locked to fixation onset in three saccade size bins

with equal number of epochs for electrode Fz. I. The same for electrode O1. J. The peak-to-peak amplitude for the saccadic spike potential and difference in amplitude between lambda and negative saccadic spike peaks for three saccade size bins. K. EEG log-power at 35 Hz time-locked to fixation onset in three saccade size bins with equal numbers of epochs for electrode Fz. L. The same for 10 Hz and electrode O1. M. Intervals of significant difference between three bins.

Figure 12. **CB dataset: Effect of saccade direction on EEG.** A. Saccade-related potential time-locked to saccade onset in the left frontal electrode F3 for four saccade directions. B. The same for the right frontal electrode F4. C. The same for electrode O1. D. EEG log-power at 35 Hz time-locked to saccade onset in the left frontal electrode F3 for four saccade directions. E. The same for the right frontal electrode F4. F. The same for electrode O1. G. Saccade duration and mean log-power at 35 Hz of saccadic spike activity in left (F3) and right (F4) frontal electrodes for four saccade directions.

Figure 13. **CB dataset: Effect of subsequent fixation duration on EEG.** A. Saccade-related potential time-locked to fixation onset in three subsequent fixation duration bins with equal numbers of epochs for electrode Fz. B. The same for electrode O1. C. EEG log-power at 10 Hz time-locked to fixation onset in three subsequent fixation duration bins with equal numbers of epochs for electrode Fz. D. The same for 10 Hz and electrode O1. E. The intervals of significant difference between three bins.

Figure 14. **Matching of eye movement characteristics.** A. Schematic illustration of matching eye movement parameters based on Mahalanobis distance. Eye movement characteristics for two hypothetical conditions are shown as data points within a large circle.

Distance of a data point from the center represents saccade size. Size of the data point marker represents fixation duration. The angular position along the circle indicates saccade direction. Mahalanobis distance of each point from the reference distribution is depicted in the color of each data point. Data points above the cutoff Mahalanobis distance are crossed out indicating elimination in the matching procedure. B. Histograms of distributions of three eye movement characteristics in conditions of central and marginal interest (see text for explanation) for one participant before and after the matching procedure.

Figure 15. **A flowchart for the combined EEG-eye movement analysis**.

Figure1

A

B

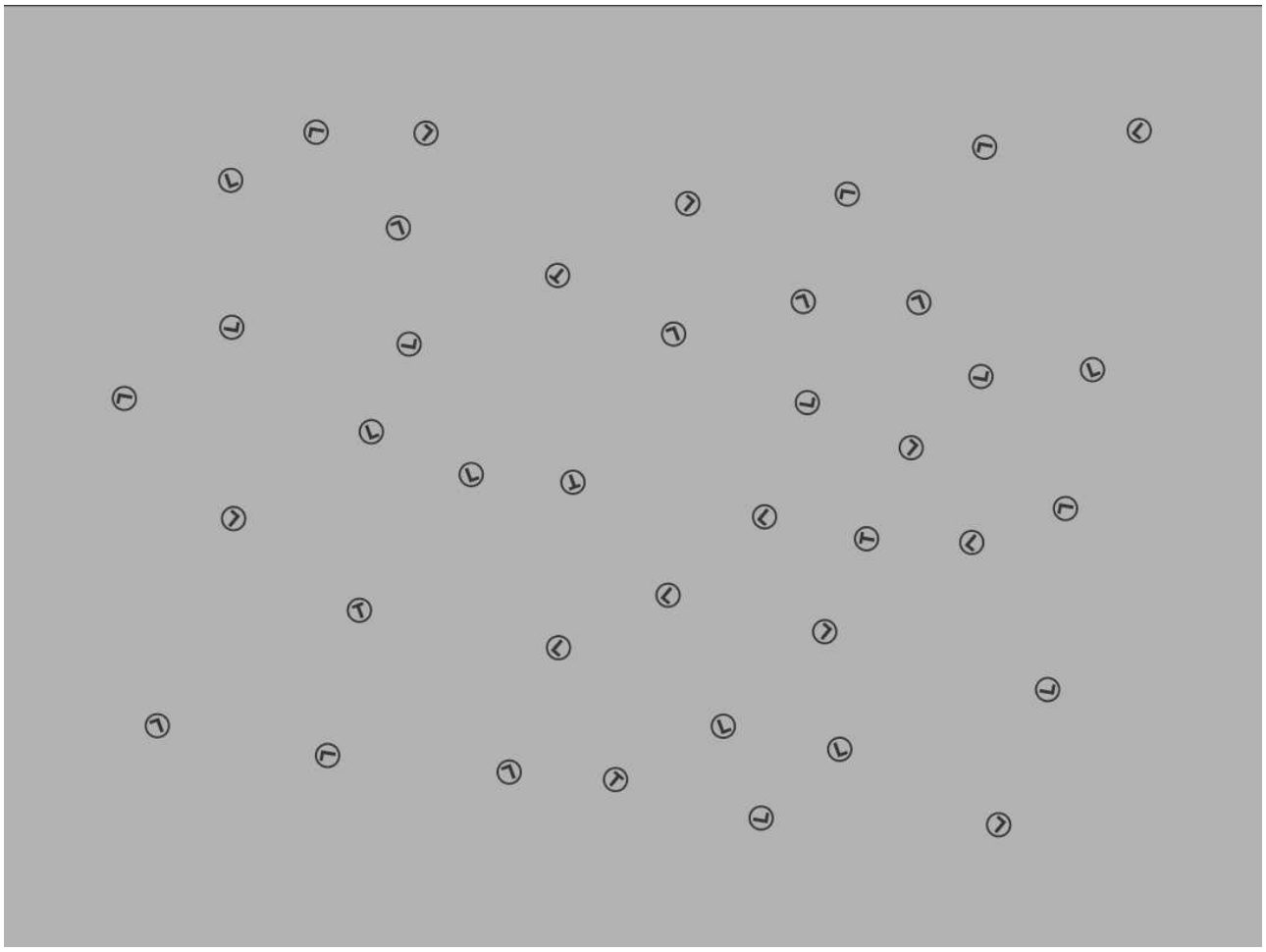

Figure2

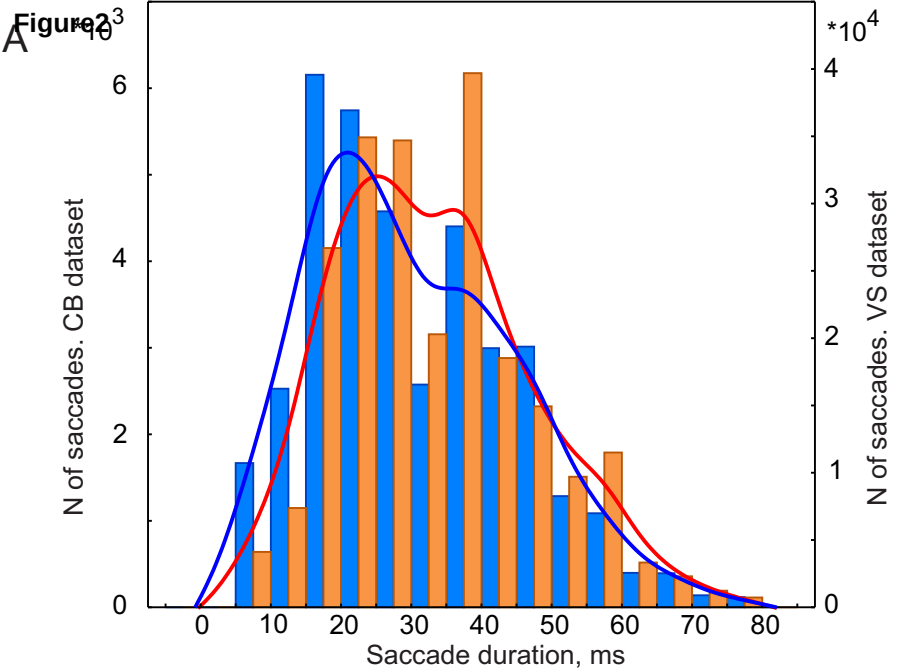
A
*10^3
6
4
2
0
N of saccades. CB dataset
*10^4
4
3
2
1
0
N of saccades. VS dataset
0 10 20 30 40 50 60 70 80
Saccade duration, ms

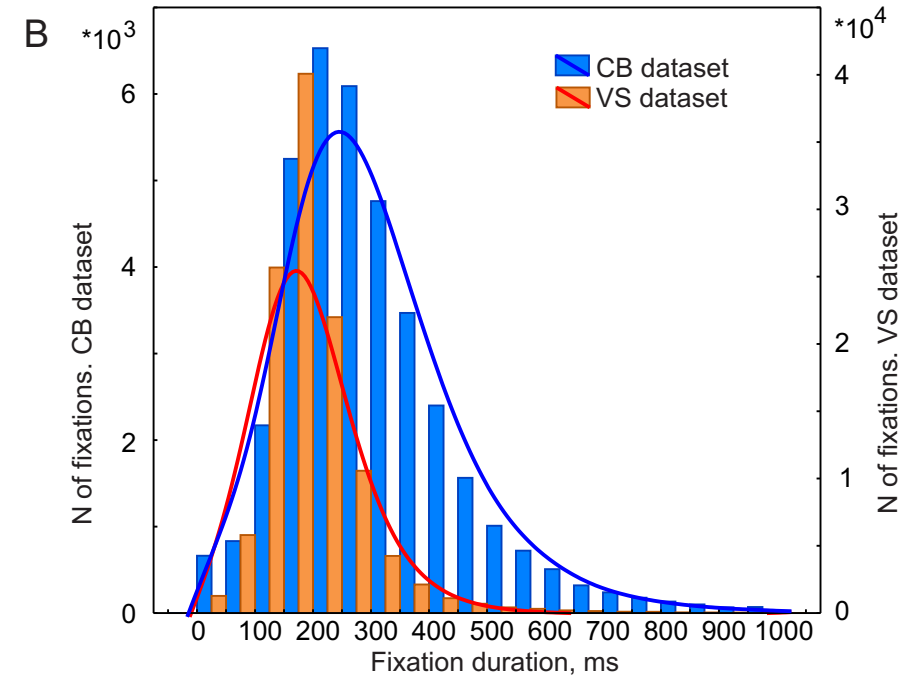
B
*10^3
6
4
2
0
N of fixations. CB dataset
CB dataset
VS dataset
*10^4
4
3
2
1
0
N of fixations. VS dataset
0 100 200 300 400 500 600 700 800 900 1000
Fixation duration, ms

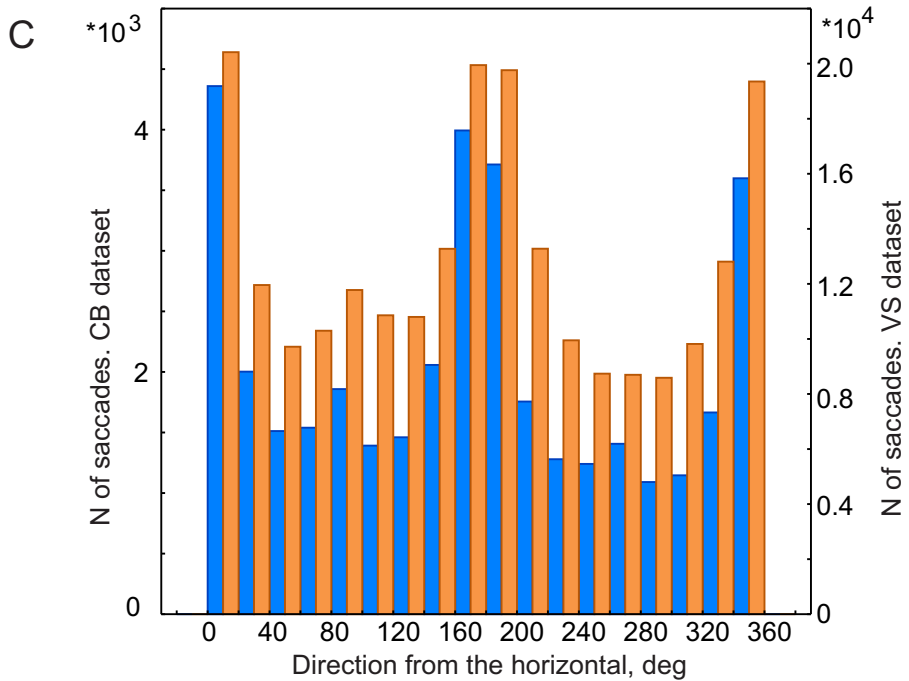
C
*10^3
4
2
0
N of saccades. CB dataset
*10^4
2.0
1.6
1.2
0.8
0.4
0
N of saccades. VS dataset
0 40 80 120 160 200 240 280 320 360
Direction from the horizontal, deg

Figure3

Click here to download high resolution image

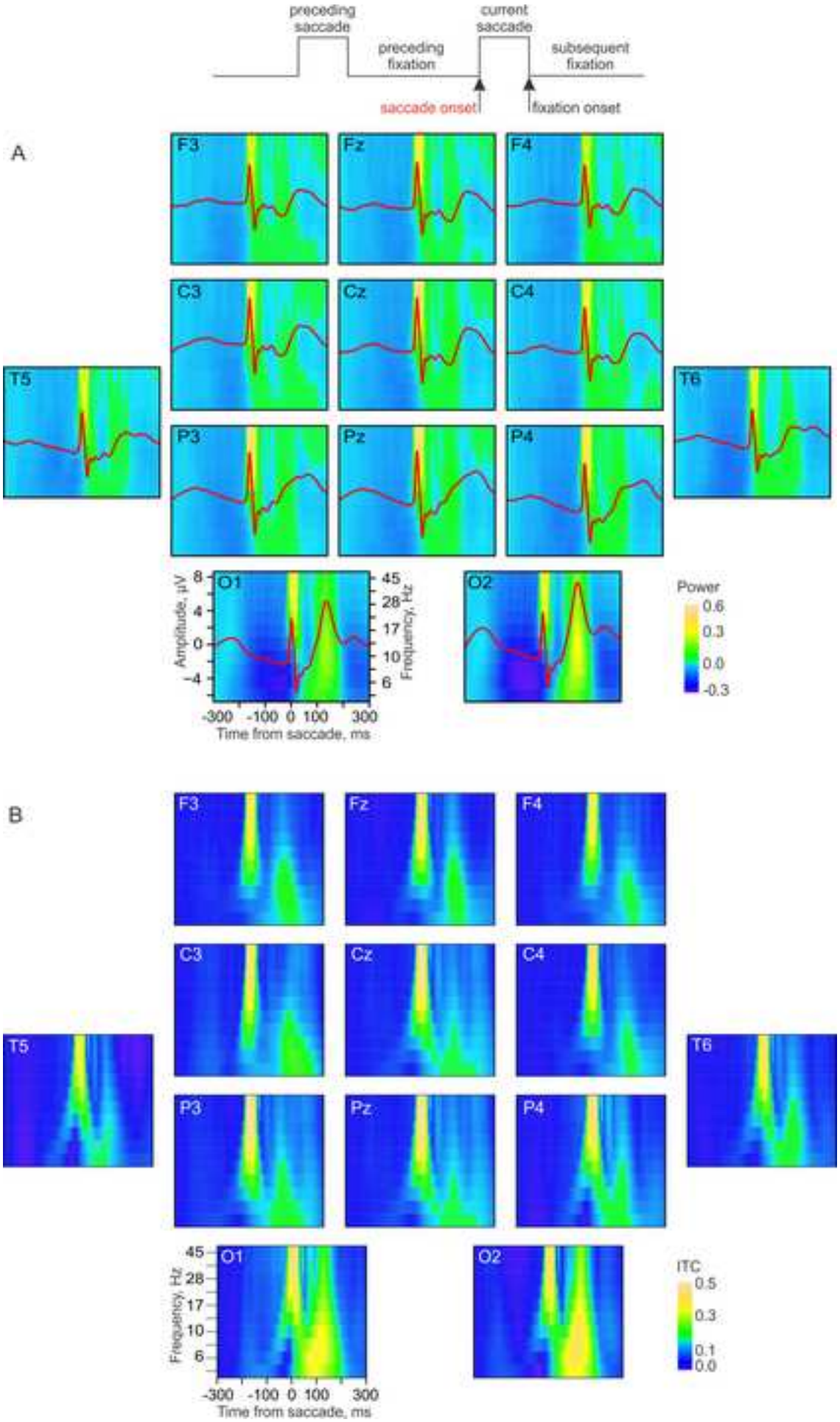

Figure4

Click here to download high resolution image

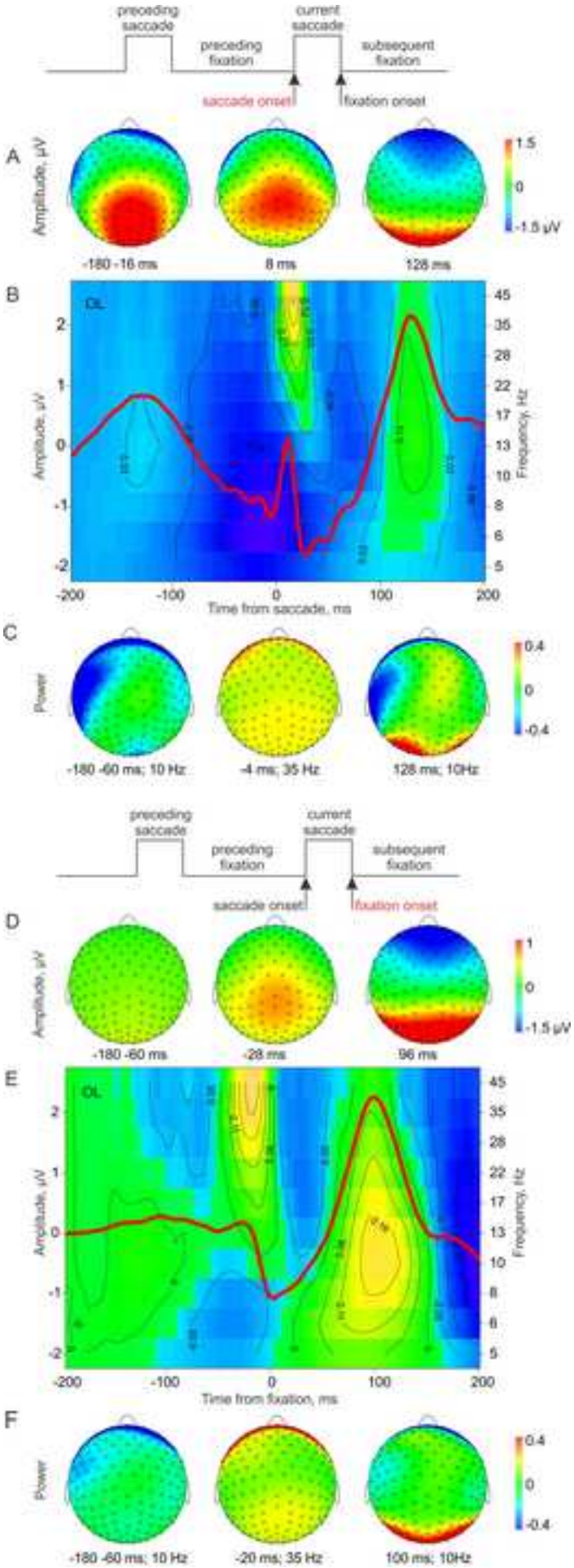

Figure5

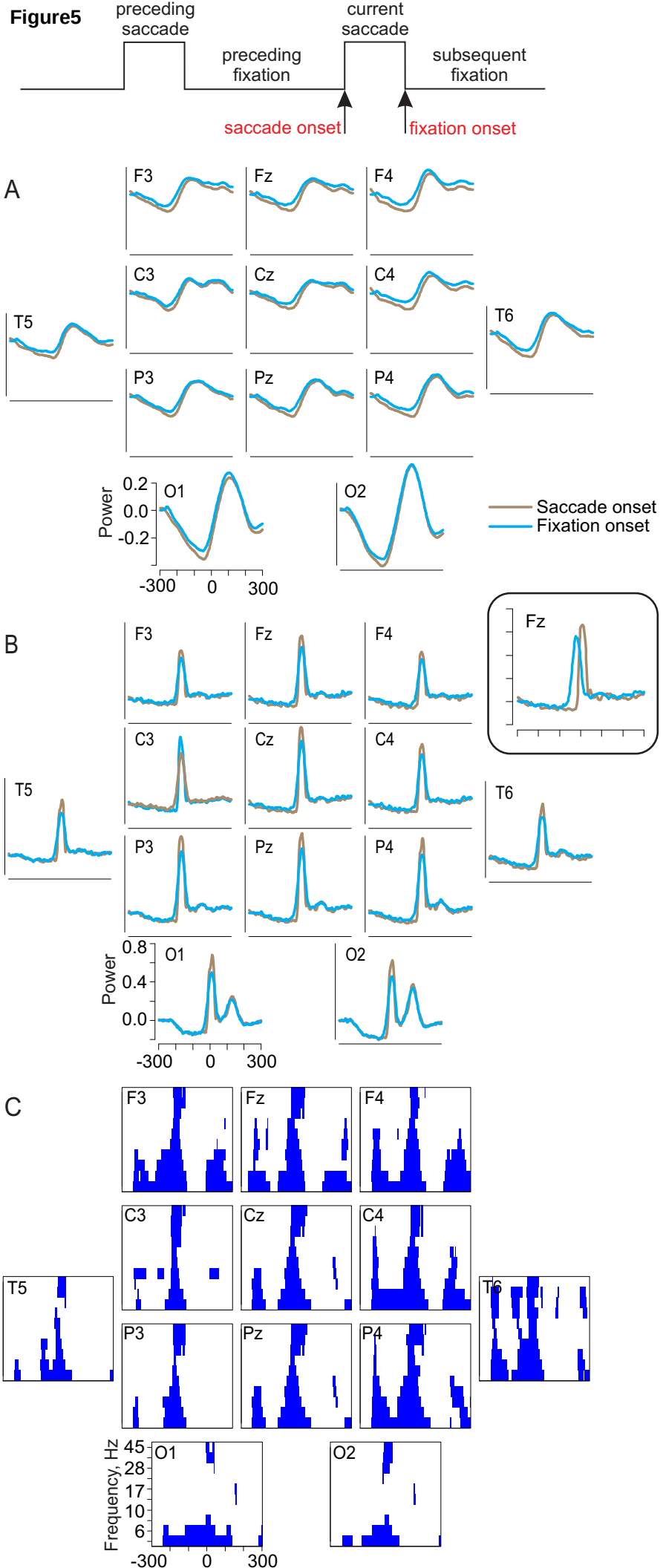
preceding saccade
current saccade
preceding fixation
subsequent fixation
saccade onset
fixation onset
A
F3
Fz
F4
C3
Cz
C4
T5
T6
P3
Pz
P4
O1
O2
Power
0.2
0.0
-0.2
-300
0
300
Saccade onset
Fixation onset
B
F3
Fz
F4
C3
Cz
C4
T5
T6
P3
Pz
P4
O1
O2
Power
0.8
0.4
0.0
-300
0
300
C
F3
Fz
F4
C3
Cz
C4
T5
T6
P3
Pz
P4
O1
O2
Frequency, Hz
45
28
17
10
6
-300
0
300

Figure6

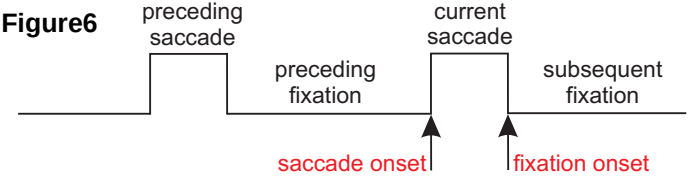
preceding saccade
current saccade
preceding fixation
subsequent fixation
saccade onset
fixation onset

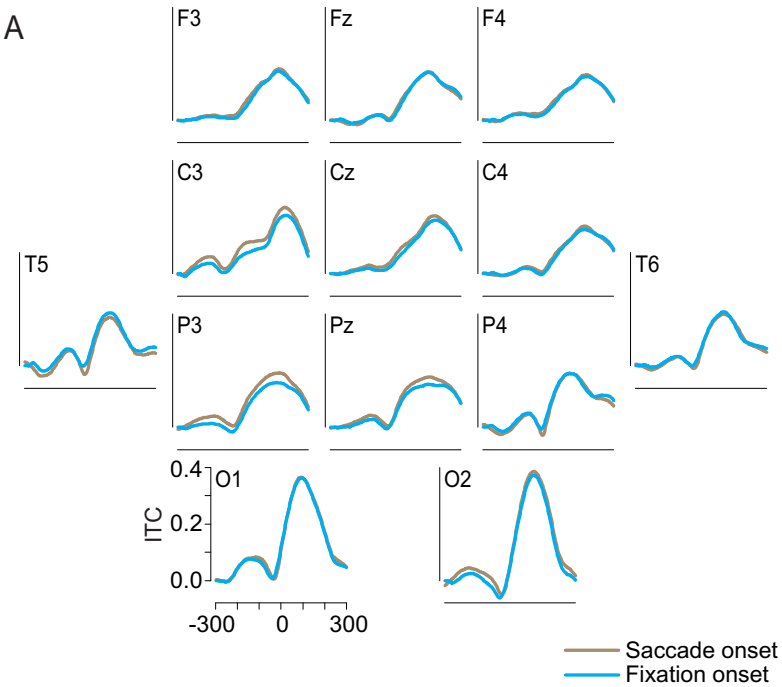
A
F3
Fz
F4
C3
Cz
C4
T5
T6
P3
Pz
P4
O1
O2
ITC
0.4
0.2
0.0
-300
0
300
Saccade onset
Fixation onset

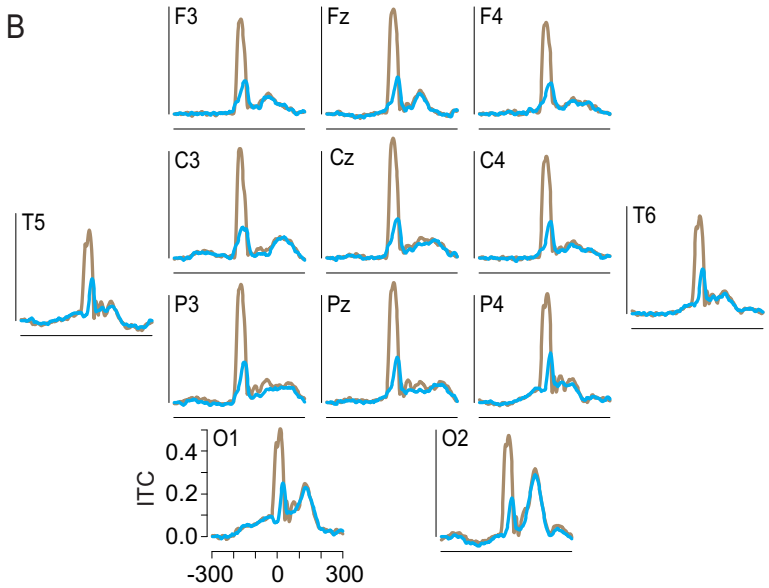
B
F3
Fz
F4
C3
Cz
C4
T5
T6
P3
Pz
P4
O1
O2
ITC
0.4
0.2
0.0
-300
0
300

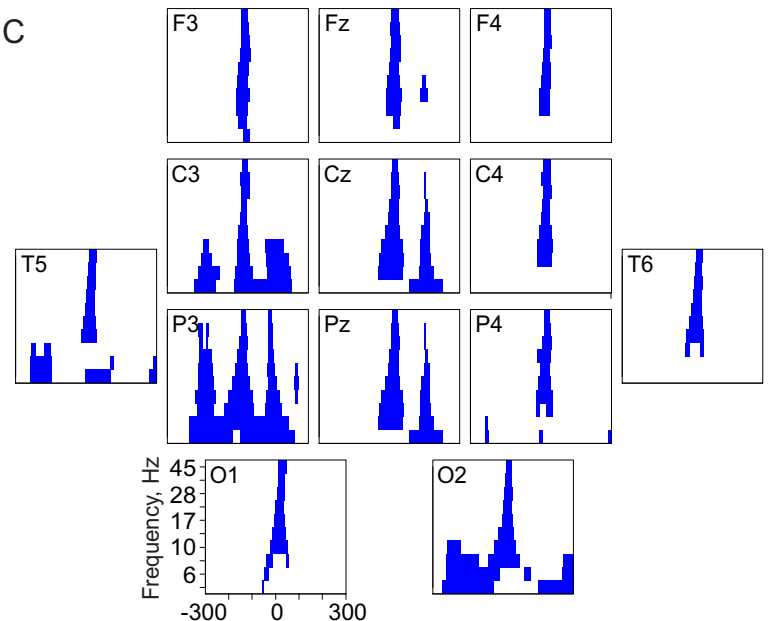
C
F3
Fz
F4
C3
Cz
C4
T5
T6
P3
Pz
P4
O1
O2
Frequency, Hz
45
28
17
10
6
-300
0
300

Figure7

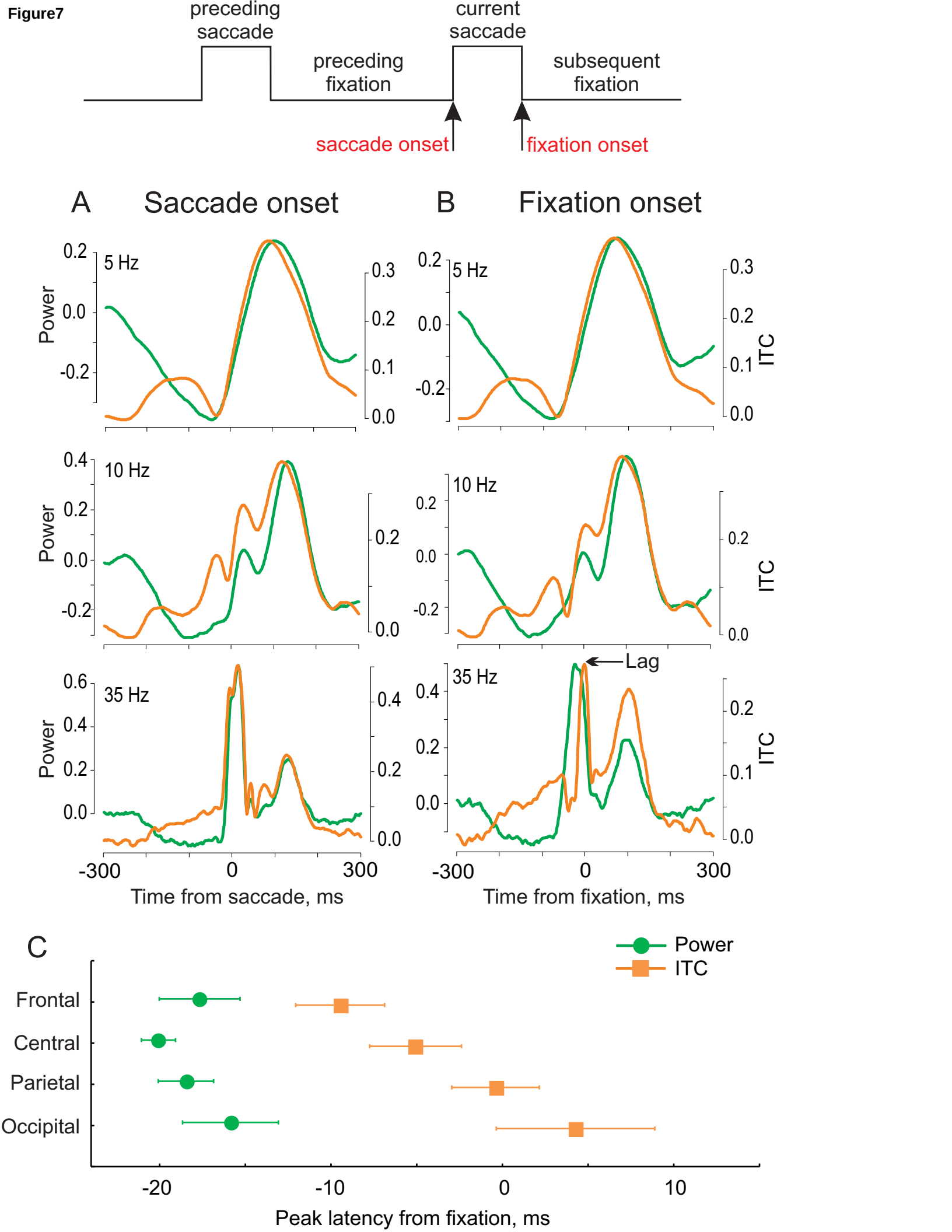
preceding saccade
current saccade
preceding fixation
subsequent fixation
saccade onset
fixation onset
A
Saccade onset
B
Fixation onset
5 Hz
10 Hz
35 Hz
Power
ITC
Lag
Time from saccade, ms
Time from fixation, ms
C
Power
ITC
Frontal
Central
Parietal
Occipital
Peak latency from fixation, ms

Figure8

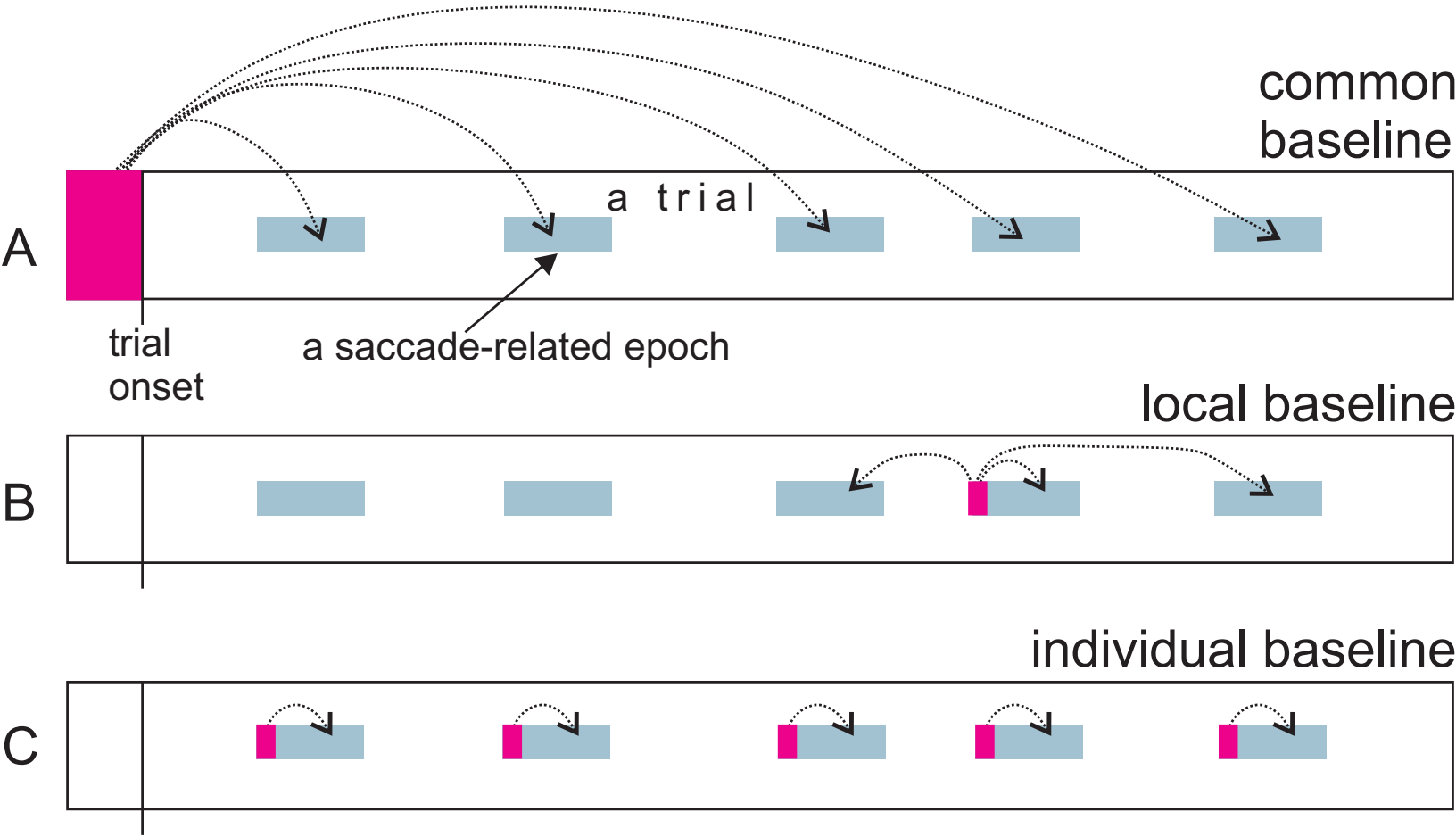
common
baseline
a trial
A
trial
onset
a saccade-related epoch
local baseline
B
individual baseline
C

Figure9

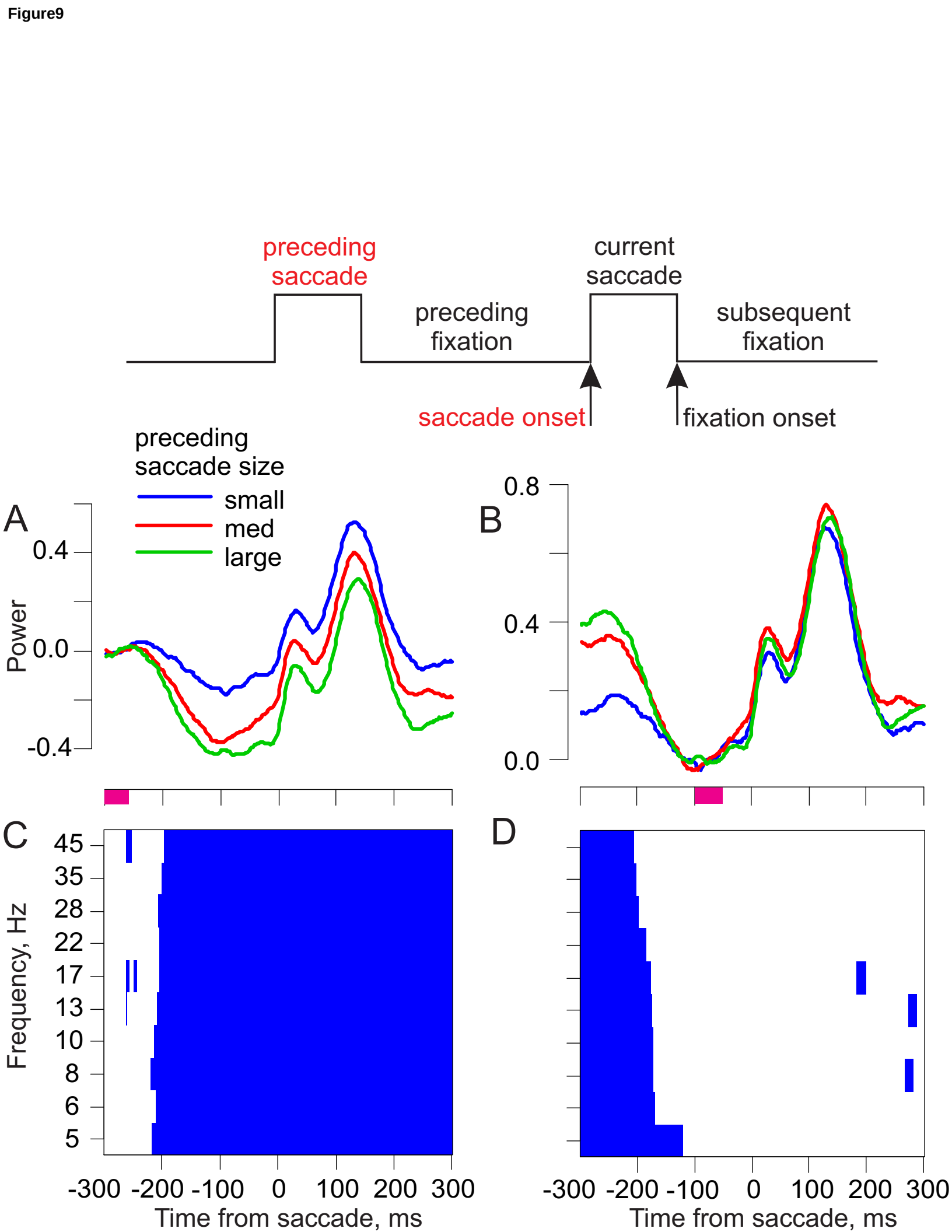
preceding saccade
current saccade
preceding fixation
subsequent fixation
saccade onset
fixation onset
preceding saccade size
small
med
large
A
B
C
D
Power
0.4
0.0
-0.4
0.8
0.4
0.0
Frequency, Hz
45
35
28
22
17
13
10
8
6
5
-300 -200 -100 0 100 200 300
Time from saccade, ms
-300 -200 -100 0 100 200 300
Time from saccade, ms

Figure10

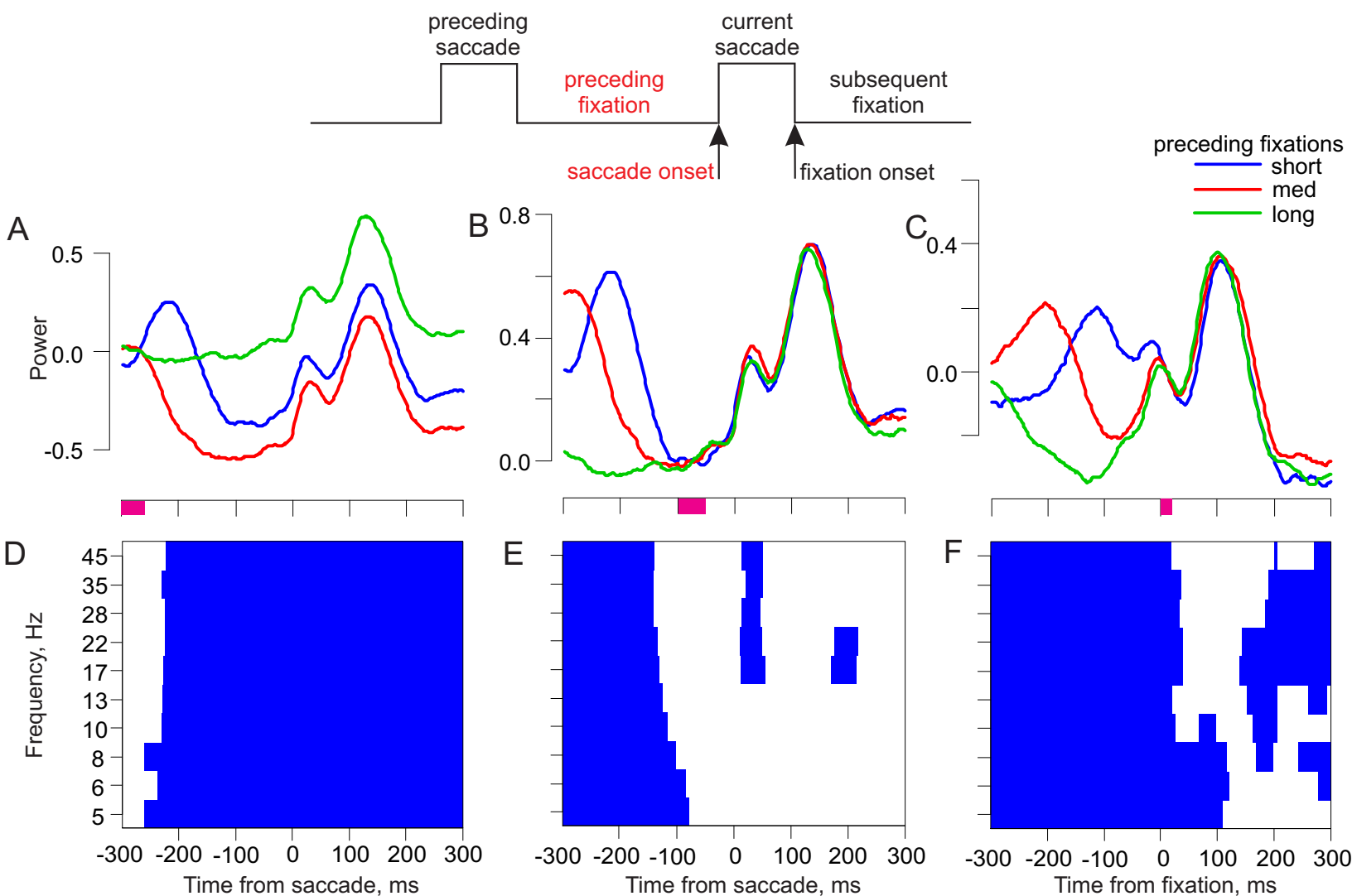
preceding saccade
current saccade
preceding fixation
subsequent fixation
saccade onset
fixation onset
preceding fixations
short
med
long
A
B
C
Power
0.5
0.0
-0.5
0.8
0.4
0.0
0.4
0.0
D
E
F
Frequency, Hz
45
35
28
22
17
13
10
8
6
5
-300 -200 -100 0 100 200 300
Time from saccade, ms
Time from saccade, ms
Time from fixation, ms

Figure11

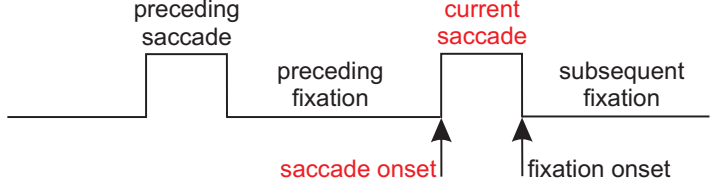
preceding saccade
current saccade
preceding fixation
subsequent fixation
saccade onset
fixation onset

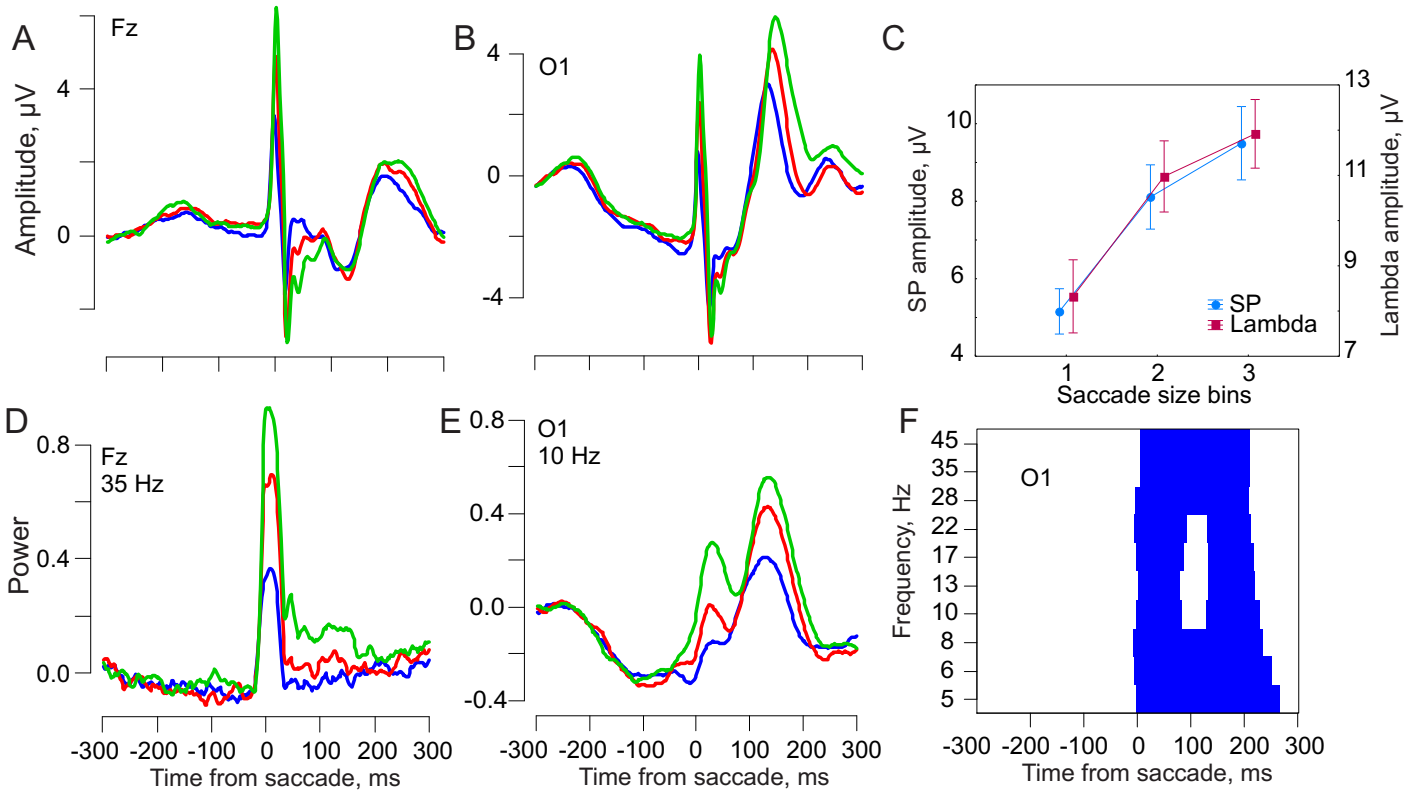
A
Fz
Amplitude, μV
B
O1
C
SP amplitude, μV
Lambda amplitude, μV
SP
Lambda
Saccade size bins
D
Fz
35 Hz
Power
Time from saccade, ms
E
O1
10 Hz
Time from saccade, ms
F
O1
Frequency, Hz
Time from saccade, ms

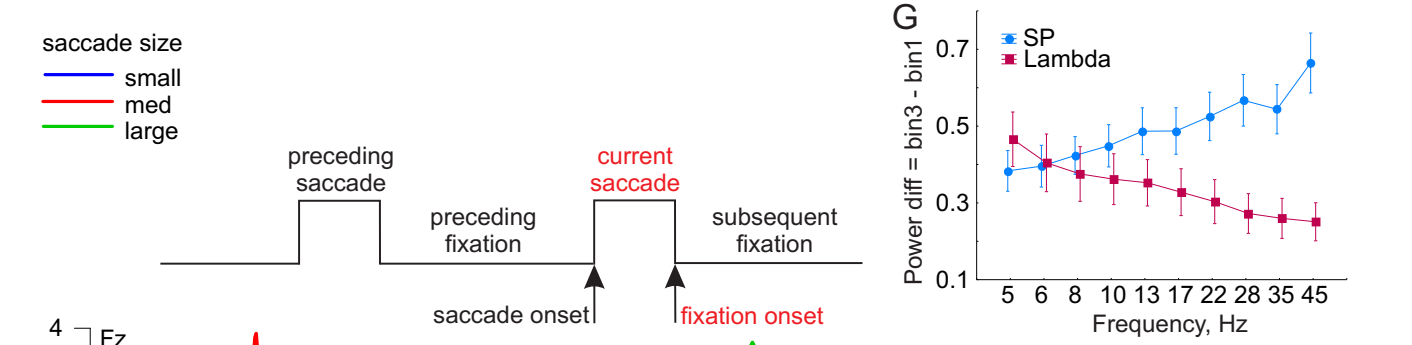
saccade size
small
med
large
G
SP
Lambda
Power diff = bin3 - bin1
Frequency, Hz

preceding saccade
current saccade
preceding fixation
subsequent fixation
saccade onset
fixation onset

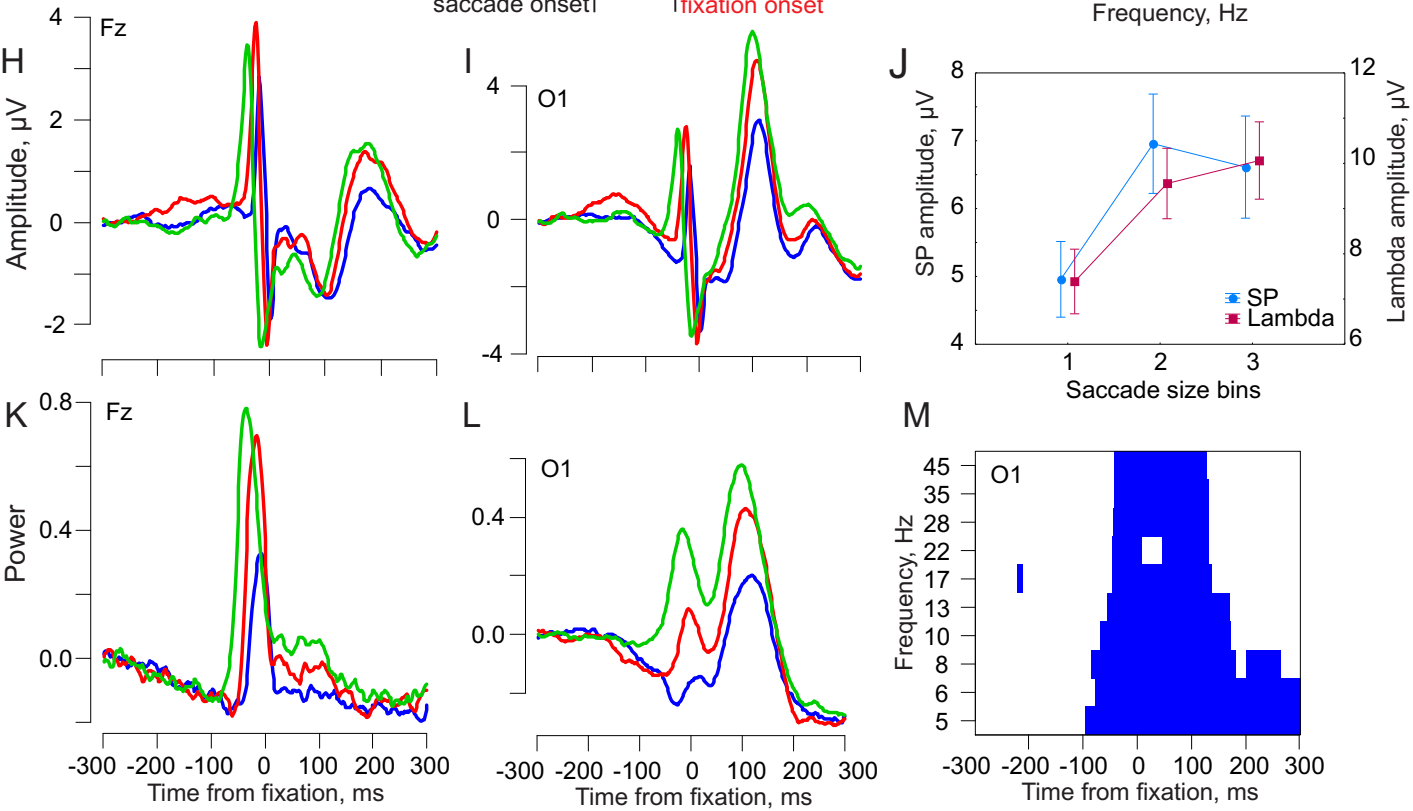
H
Fz
Amplitude, μV
I
O1
J
SP amplitude, μV
Lambda amplitude, μV
SP
Lambda
Saccade size bins
K
Fz
Power
Time from fixation, ms
L
O1
Time from fixation, ms
M
O1
Frequency, Hz
Time from fixation, ms

Figure12

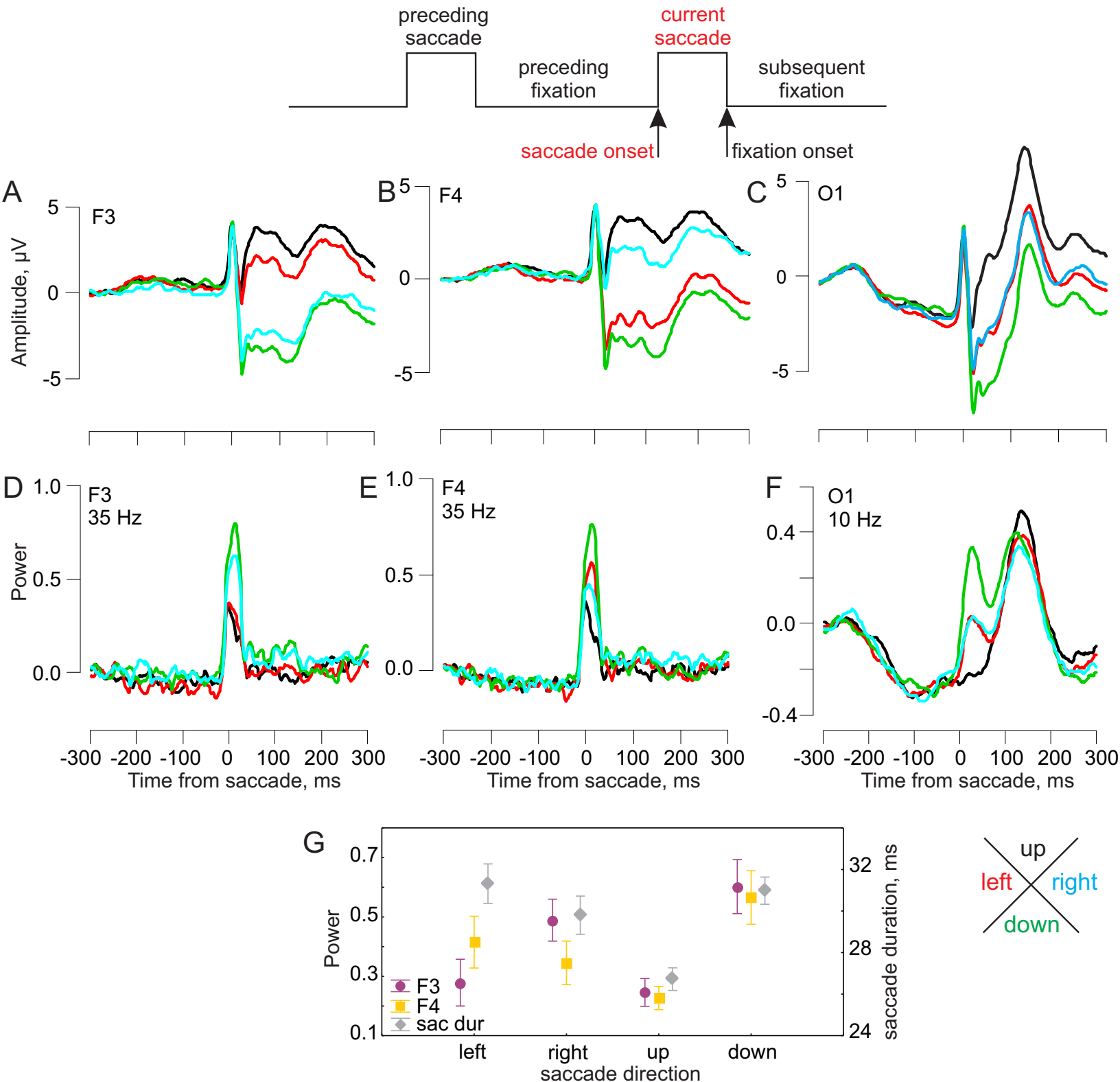
preceding saccade
current saccade
preceding fixation
subsequent fixation
saccade onset
fixation onset
A
F3
B
F4
C
O1
Amplitude, μV
5
0
-5
D
F3
35 Hz
E
F4
35 Hz
F
O1
10 Hz
Power
1.0
0.5
0.0
0.4
-0.4
-300 -200 -100 0 100 200 300
Time from saccade, ms
G
0.7
0.5
0.3
0.1
32
28
24
saccade duration, ms
F3
F4
sac dur
left
right
up
down
saccade direction
up
left
right
down

Figure12

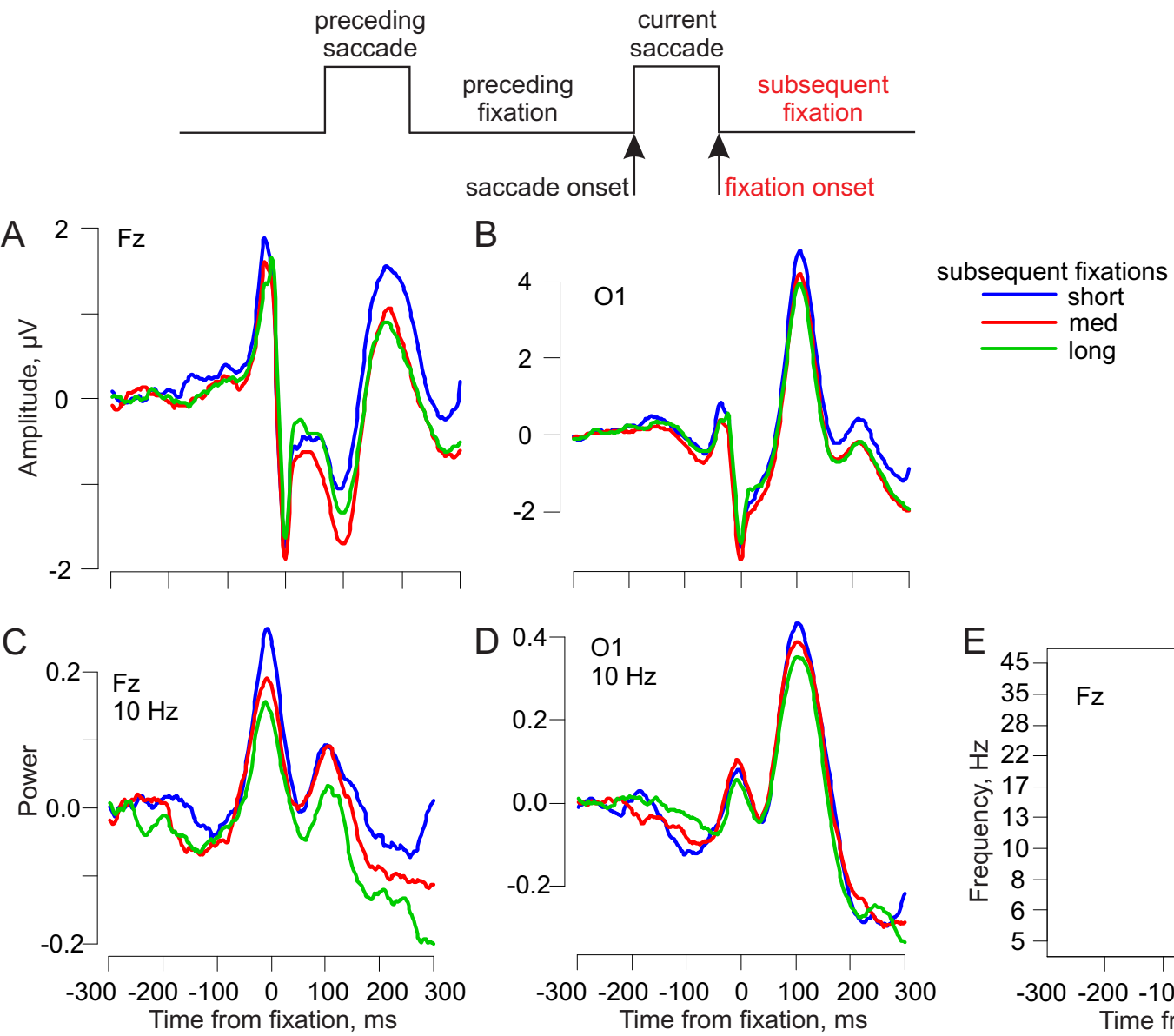
preceding saccade
current saccade
preceding fixation
subsequent fixation
saccade onset
fixation onset
A
Fz
Amplitude, μV
2
0
-2
B
O1
4
2
0
-2
subsequent fixations
short
med
long
C
Fz
10 Hz
Power
0.2
0.0
-0.2
-300 -200 -100 0 100 200 300
Time from fixation, ms
D
O1
10 Hz
0.4
0.2
0.0
-0.2
-300 -200 -100 0 100 200 300
Time from fixation, ms
E
Fz
Frequency, Hz
45
35
28
22
17
13
10
8
6
5
-300 -200 -100 0 100 200 300
Time from fixation, ms

Figure14

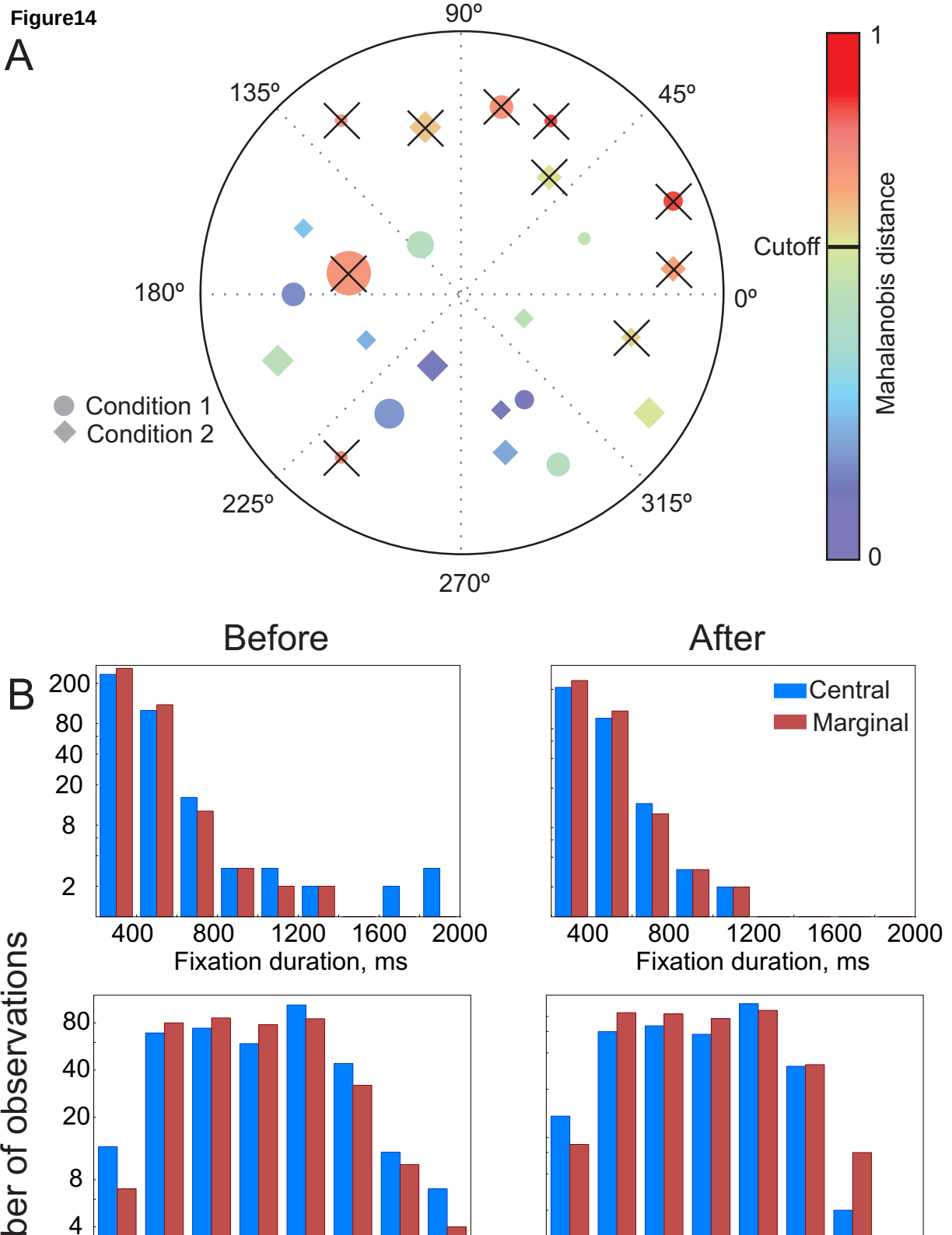
A
90°
135°
45°
180°
0°
225°
315°
270°
Condition 1
Condition 2
Cutoff
1
0
Mahalanobis distance

Before
After
B
Central
Marginal
Fixation duration, ms
Saccade duration, ms
Saccade direction, deg
Number of observations

Figure15

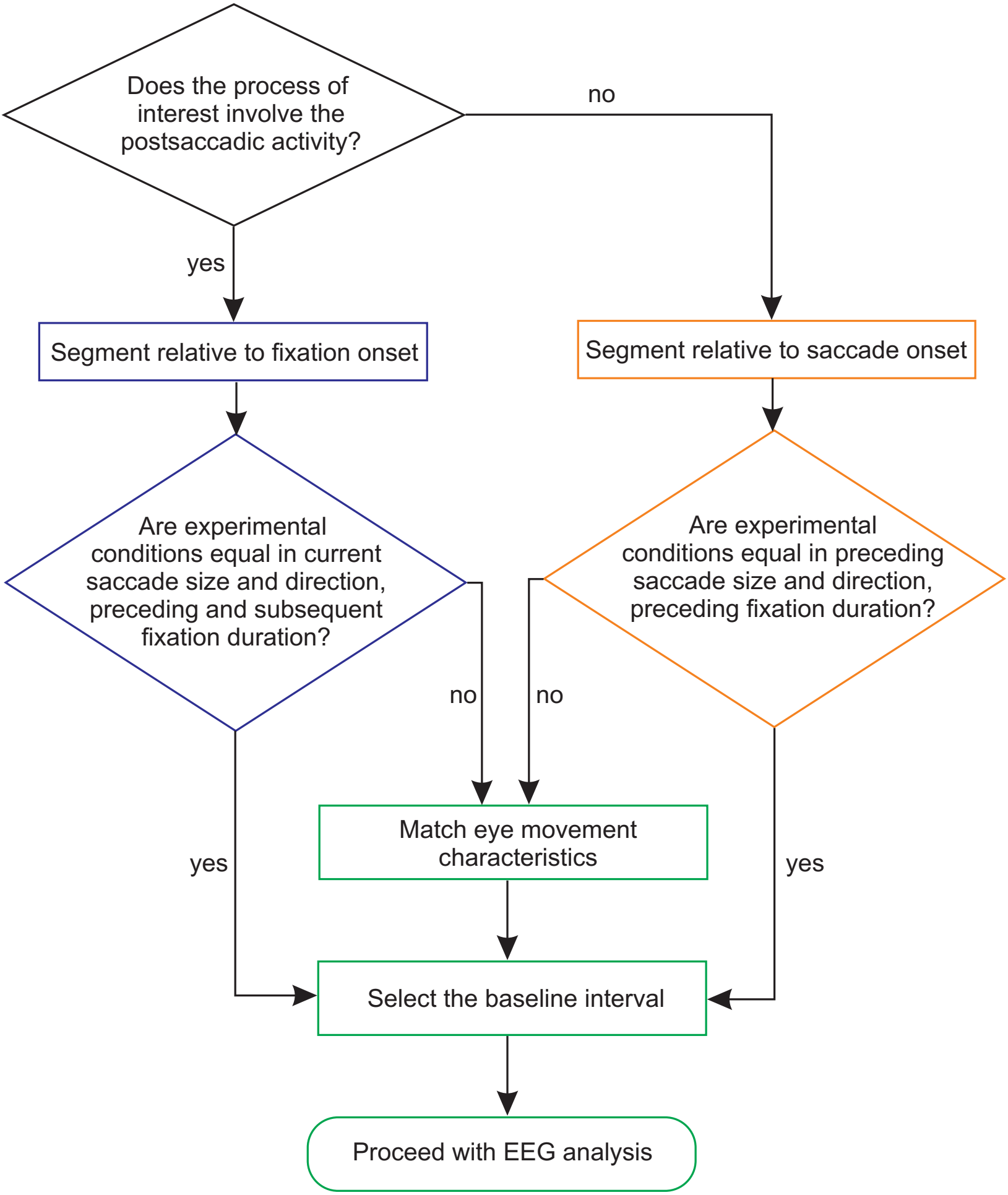
Does the process of interest involve the postsaccadic activity?
no
yes
Segment relative to fixation onset
Segment relative to saccade onset
Are experimental conditions equal in current saccade size and direction, preceding and subsequent fixation duration?
Are experimental conditions equal in preceding saccade size and direction, preceding fixation duration?
no
no
yes
yes
Match eye movement characteristics
Select the baseline interval
Proceed with EEG analysis